Demonstration of Network Level Pavement Structural Evaluation with Traffic Speed Deflectometer in Virginia

Prepared for **the Federal Highway Administration**
Under Contract # DTFH61-11-D-00009-T-13008

By

Virginia Tech Transportation Institute

Subcontractor to

Engineering & Software Consultants, Inc.

July 2017

TABLE OF CONTENTS

<table>
<tr><td>Report No.:</td><td>Report Date:
July 2017</td><td>No. Pages:
41</td><td>Type Report:
Final Contract</td><td>Project No.:</td></tr>
<tr><td colspan="3" rowspan="2"></td><td>Period Covered:
October 2013 – February 2017</td><td>Contract No.:
DTFH61-11-D-00009-T-13008</td></tr>
<tr><td colspan="4">Title:
Demonstration of Network Level Structural Evaluation with Traffic Speed Deflectometer in Virginia</td><td rowspan="3">Key Words:
Traffic Speed Deflectometer, Deflection Testing, Non-Destructive Evaluation, Network-Level Decision Making, Structural Capacity Index</td></tr>
<tr><td colspan="4">Author(s): Samer Katicha*, Ph.D., Gerardo Flintsch*, Ph.D., P.E., Shivesh Shrestha*, and Senthilmurugan Thyagarajan**, Ph.D.</td></tr>
<tr><td colspan="4">Performing Organization Name and Address:
Prime Contractor: Engineering & Software Consultants, Inc. (ESCINC)
14123 Robert Paris Court
Chantilly, VA 20151

Subcontractor: Virginia Tech Transportation Institute (VTTI)
3500 Transportation Research Plaza
Blacksburg, VA 24061</td></tr>
<tr><td colspan="5">Sponsoring Agencies' Name and Address:
Office of Infrastructure Research and Development
Federal Highway Administration
6300 Georgetown Pike
McLean, VA 22101-2296
and the State Department of Transportation of the States of California, Georgia, Idaho, Illinois, Nevada, New York, Pennsylvania, South Carolina and Virginia</td></tr>
<tr><td colspan="5">Supplementary Notes:
The Contracting Officer's Representative was Nadarajah Sivaneswaran, HRDI-20.
* affiliated with VTTI; ** affiliated with ESCINC</td></tr>
<tr><td colspan="5">Abstract:
The objective of this transportation pooled fund study was to carry out a field demonstration of the Traffic Speed Deflectometer (TSD) and present an approach of how the results of TSD testing could be implemented within a pavement management system (PMS). This report summarizes the results of this field demonstration effort in Virginia. Specifically this report 1) describes the TSD and its measurement approach, 2) presents the structural condition of the tested roads as part of the demonstration, 3) evaluates the repeatability of the TSD on two sections, 4) compares TSD measurement Falling Weight Deflectometer (FWD), 5) compares TSD structural condition with information obtained from the PMS, 6) shows how the information obtained from the TSD can be used from a simple relative ranking of the pavement structural condition to more elaborate approaches that calculate different indices (e.g. SCI300, effective structural number (SN_{eff}), tensile strain at the bottom of the asphalt layer), and 7) shows how the TSD measurements can be incorporated into a PMS decision process.
A companion report summarizes the results from transportation pooled fund study in all nine states. The companion report also contains information on interpreting files associated with TSD data, data processing method used in the study and Profilograph program to view the TSD data.</td></tr>
</table>

FIELD DEMONSTRATION OF THE TSD IN VIRGINIA

Samer Katicha[1], Gerardo Flintsch[1], Shivesh Shrestha[1], and Senthilmurugan Thyagarajan[2]

INTRODUCTION

This report describes the results of the Traffic Speed Deflectometer (TSD) demonstration performed in Virginia from June 15 to June 17, 2015, and how the results of the TSD testing can be implemented into the Virginia Pavement Management System (PMS). The focus in this report is on practical implementation of the TSD for production testing on flexible pavement sections with unbound bases (for an investigation that is more focused on accuracy and repeatability, Rada et al. 2016 and Flintsch et al. 2013 are recommended along with the references therein). As the research effort described in this report is part of a pooled fund study with nine state highway agencies participating, a separate report that highlights the results from the overall research effort was prepared and distributed to the nine participating states and will be posted to the pooled fund website. The focus of this report is on the results of tests performed in Virginia and on answering the following important questions:

1. **What is the TSD and what does it measure?** The TSD data collection method and recorded measurements are different from those of the more familiar Falling Weight Deflectometer (FWD). The TSD is a continuously moving device that measures the instantaneous pavement vertical velocity under a moving load, whereas the FWD is a stationary device that measures the time history of the pavement's vertical velocity or acceleration at each sensor. The TSD reports instantaneous deflection slopes, while the FWD reports maximum deflections. This report presents the measuring principle of the TSD along with how deflection basin indices, including asphalt strain, can be estimated from the TSD measurements. The method of Rada et al. (2016) to temperature correct the estimated tensile strain at the bottom of the asphalt layer form TSD measurements is also presented.

2. **What is the structural condition of the tested roads?** This report presents the pavement structural condition of the tested roads in terms of the SCI300 surface curvature index (SCI) corrected to a reference temperature of 70°F (21.1°C) using the procedure developed by Rada et al. (2016). This includes SCI300 box plots of the roads tested, typical line plots of SCI300 versus distance, and Google Earth color-coded plots (good, fair, and poor). The colors used are green, yellow, and red to represent good, fair, and poor structural conditions. The thresholds used to classify the condition are based on the estimated remaining fatigue life of the asphalt layer. Using typical default average daily truck traffic (ADTT) levels for interstate, primary, and secondary roads, and typical

[1] Virginia Tech Transportation Institute
[2] Engineering & Software Consultants, Inc.

thicknesses (the method can be improved with section specific thickness), sections with an estimated remaining fatigue life less than 2 years are considered to have a poor structural condition, those with an estimated remaining fatigue life of between 2 and 5 years are considered fair, and those with an estimated remaining fatigue life more than 5 years are considered good. These thresholds are provided as initial default estimates, and it is recommended that each state highway agency adjust the thresholds to best represent their pavements and to meet their pavement management needs.

3. **How repeatable are TSD measurements?** Repeatability was estimated by comparing temperature-corrected SCI300 measurements performed on the same sections.

4. **How do TSD measurements compare with FWD?** TSD measurements were compared with FWD measurements to determine if the two devices showed similar trends in measured values along the tested sections. There are a number of differences between the TSD and FWD that lead to the two devices giving different measurement magnitudes. Some of the most important differences are (1) the TSD applies a rolling load on the pavement, while the FWD applies an impact load on the pavement; (2) the TSD load is applied through flexible dual tires but the FWD load is applied through a rigid plate; (3) the TSD measurements from all sensors are obtained at the same time whereas the FWD measurements are the peak deflections from each sensor, which do not occur at the same time (the peaks from sensors farther away from the loaded area occur at a later time compared to the peak from sensors closer to the loaded area) and (4) the TSD makes continuous measurements and report average values at 10m intervals while FWD measurement are made at discrete locations. Other issues that arise when comparing TSD and FWD measurements pertain to the fact that the two sets of measurements were obtained at different times and different pavement temperatures. Although temperature correction can be applied, the correction is based on empirical equations and therefore only approximate. For these reasons, the comparison between the two devices in this report is limited to comparing trends and evaluating to what extent the two devices identified the same weak sections.

5. **How do TSD measurements compare with PMS data?** TSD measurements were also compared with pavement condition data on interstate roads. Special attention was given to comparing the TSD SCI300 with observed pavement fatigue cracking, with the comparison showing in general a weak relationship, suggesting TSD measurements provide information on the pavement structural condition that cannot be inferred from observed surface cracking in particular and more generally observed surface condition.

6. **How can we use the information obtained from TSD measurements?** Information from TSD measurements can help to better manage pavement sections. The best way to use TSD data mostly depends on each agency's approach to managing its pavement sections. In the short term, TSD data can be used to verify and/or adjust the decisions that

are largely based on surface condition. TSD measurements can readily be used to obtain a relative ranking between different pavement sections or, with the use of appropriate thresholds, to identify structurally good, fair, and poor segments. When pavement thickness data are available, a more mechanistic approach can be used to estimate tensile strains at the bottom of the asphalt layer and a fatigue equation can be used to estimate remaining fatigue life. All these approaches are presented in detail in this report.

7. **How can we incorporate TSD measurements into a PMS?** The proposed approach to incorporate TSD into the PMS (for flexible pavements) consists of classifying the pavement structural condition into Good, Fair, and Poor categories based on temperature-corrected structural indices derived from TSD measurements. Both SCI300 and the Deflection Slope Index (DSI) were investigated. The results showed that similar conclusions are drawn whether SCI300 or DSI is used; therefore, only the results of SCI300 are presented in this report (results with DSI are provided in the Excel files). Preliminary thresholds that separate between the Good, Fair, and Poor structural condition categories are given in this report based on an estimate of the expected remaining fatigue life of the asphalt layer. This expected remaining fatigue life is related to the tensile strain at the bottom of the asphalt layer, which in turn is related to the SCI300 (or DSI) using the approach developed in Rada et al. (2016). It is recommended that each agency calibrate these thresholds based on their own experience and needs. Since the Virginia Department of Transportation (VDOT) already use structural condition information for Interstate roads, a possible approach to perform the calibration would be to adjust the Good, Fair, and Poor thresholds used with the TSD SCI300 so that final treatment decision obtained with TSD data match as closely as possible with final treatment decisions obtained with FWD data. An illustration of decision process is provided to illustrate how structural condition can be used in the PMS.

Why Measure the Structural Condition of the Pavement?

Pavement structural capacity has a big effect on the rate of pavement deterioration. In turn, the rate of deterioration of pavement sections is used to estimate the time and type of maintenance activities in a PMS. Due to (until recently) the relative difficulty of measuring the pavement structural condition at the network level, traditional PMS approaches have relied on observation of the pavement surface condition to assess rehabilitation needs. However, the pavement surface condition does not provide a full picture of the causes of deterioration; it is only the symptom. This has been confirmed by a number of studies that showed that the correlation between surface condition and structural measurements of pavement response is weak (Flora, 2009; Bryce et al., 2013) and that the rate of deterioration of pavement sections is affected by the structural condition (Katicha et al., 2016). Therefore, the pavement structural condition is an important aspect of overall pavement health and one of the driving causes of pavement deterioration.

The fact that the structural condition is an important factor alone may not be convincing enough for a highway agency to invest the resources to implement the TSD for network-level pavement structural assessments. Any such endeavor would first have to be justified from an economic perspective that demonstrates that the benefits of incorporating reliable pavement structural condition information in pavement management decision making far outweigh the data collection costs. The pooled fund study whose results are documented in this report grew from the belief that there is enough evidence in the literature that the TSD is a device that could provide valuable pavement structural information at relatively lower cost than deploying the FWD at the network level (Flintsch et al. 2013; Rada et al., 2016). In that respect, the Federal Highway Administration (FHWA) initiated the pooled fund project "*Demonstration of Network Level Pavement Structural Evaluation with Traffic Speed Deflectometer*" to assess the feasibility and demonstrate the use of the TSD for network-level pavement structural evaluation for use in the participating agencies' pavement management application and decision making. This report summarizes the testing performed in the state of Virginia in terms of the research questions presented in the introduction.

RESEARCH QUESTION 1: WHAT IS THE TSD AND WHAT DOES IT MEASURE?

The TSD, shown in Figure 1, is an articulated truck with a rear-axle load that can be varied from 58.7 to 127.6 kN (13,196 to 28,686 lbf) by using sealed lead loads. The TSD has a number of Doppler lasers mounted on a servo-hydraulic beam to measure the deflection velocity of a loaded pavement. The TSD evaluated in this study used seven Doppler lasers. Six Doppler lasers were positioned such that they measure deflection velocity at 100, 200, 300, 600, 900, and 1,500 mm (3.9, 7.9, 11.8, 23.6, and 59 inches) in front of the loading axle. The seventh sensor was positioned 3,500 mm (11.5 ft) in front of the rear axle, largely outside the deflection bowl, to act as a reference laser. The beam on which the lasers are mounted moves up and down in opposition to the movement of the trailer in order to keep the lasers at a constant height from the pavement's surface. To prevent thermal distortion of the steel measurement beam, a climate control system maintains the trailer temperature at a constant 20°C (68°F). Data are recorded at a survey speed of up to 96 km/h (60 mph) at a rate of 1000 Hz.

Figure 1. Picture of TSD used during testing and computer-generated schematic.

Measurement Technology

The TSD uses Doppler lasers mounted at a small angle to the vertical to measure the overall velocity that comprises the following components: 1) vertical pavement deflection velocity, 2) horizontal vehicle velocity, and 3) vertical and horizontal vehicle suspension velocity. Due to its location, midway between the loaded trailer axle and the rear axle of the tractor unit, the pavement under the reference laser is expected to be outside the zone of load influence (undeformed). Its response is therefore used to remove the unwanted vertical and horizontal vehicle suspension velocity from the six measurement lasers. The horizontal velocity is also measured independently and used to determine the horizontal component of the velocity measured by the Doppler lasers. With horizontal component of the velocity known, the vertical velocity of the pavement deflection is determined (see Figure 2). To remove the effect of the vehicle speed, the deflection velocity is divided by the instantaneous vehicle speed to give a measurement of deflection slope, as illustrated in the Figure 2. Therefore, the deflection slope is calculated as follows:

$$S = \frac{V_v}{V_h} \tag{1}$$

where S is the deflection slope, V_v is the vertical pavement deflection velocity, and V_h is the vehicle horizontal velocity. Typically, the deflection velocity is measured in mm/s and the vehicle speed is measured in m/s; therefore, the deflection slope measurements are output in units of mm/m and generally reported at a 10-m (33-ft) interval. At a speed of 80 km/h (50 mph) and a data collection frequency of 1000 Hz, this corresponds to an average of 446 individual measurements over the 10 m section.

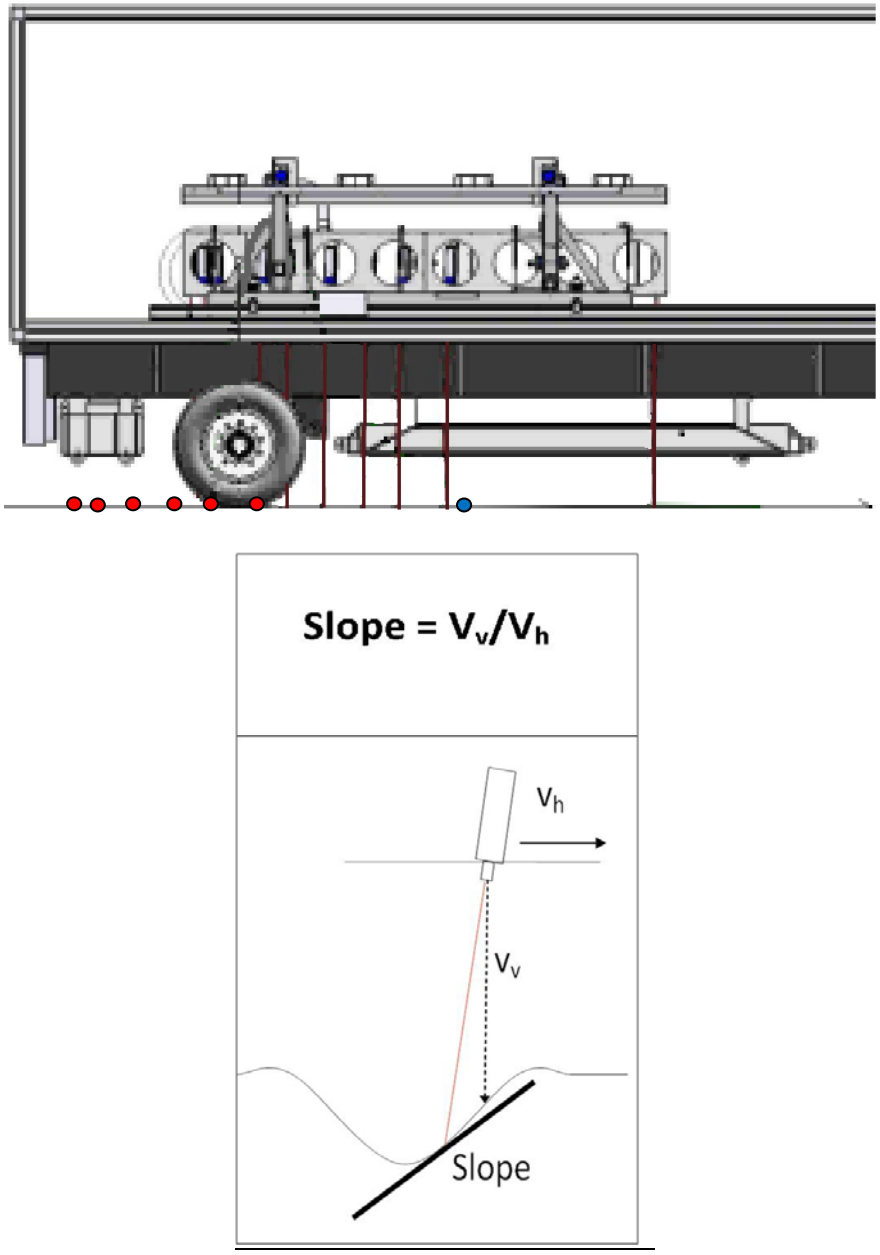

Figure 2. Schematic of the measurement principle of the TSD.

Relationship between Deflection Slope, Deflection, and Other Pavement Structural Condition Indices

As described, the TSD measures the deflection slope of the deflection basin rather than pavement deflection. Figure 3 shows how the deflections and deflection slopes relate to the deflection basin. The deflection basin represents the profile of the deflected pavement. The deflection at a position on the deflection basin is the vertical distance from that point to the reference undeformed pavement. The deflection slope is the tangent to the deflection basin (i.e., the derivative of the

deflection basin). Since the deflection slope is the derivative of the deflection, the deflection can be obtained from the deflection slope by integration as follows:

$$d(x) = \int_x^{\infty} s(y)dy \qquad (2)$$

where,

$s(y)$ = slope at distance y measured from the applied load;

$d(x)$ = deflection at distance x measured from the applied load.

Greenwood engineering uses a parametrized model for the shape of the deflection slope developed by Pedersen et al. (2013) to obtain deflections from the deflection slope by optimizing the model parameters to fit the deflection slope data. The deflections computed from this model are reported in the data file (with extension .tsd.tsddefl.xls) and are used in this report.

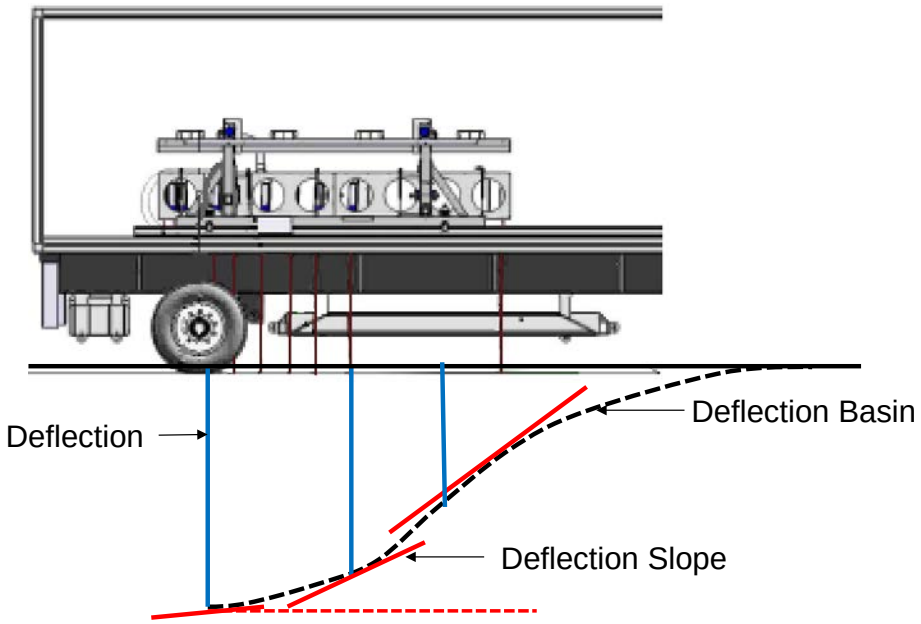

Figure 3. Relationship between the deflection basin, deflection, and deflection slope.

While deflections can directly be used to infer the structural condition and capacity of the tested pavement, a number of studies have shown that deflection-basin-related indices correlate better to the pavement responses that cause load-related distresses (Horak, 1987; Thyagarajan et al., 2011).

What Are Deflection-Basin-Related Indices?

Deflection-basin related indices are indices that are computed from two or more measured deflections . One of the widely used indices with the FWD is SCI300, which is the difference between the deflection under the applied load (i.e., D0) and the deflection 300 mm (12 in.) from the applied load (i.e., D300), shown in Equation 3.

$$SCI300 = D0 - D300 \quad (3)$$

The SCI300 can also be calculated from TSD measurements using the calculated deflections. However, it is very important to point out that while the TSD and FWD both attempt to measure the same metric—pavement structural condition—they are different in how they apply the load and record the pavement response. Although the SCI300 (or any other parameter) obtained from each device would qualitatively agree and have similar trends, quantitatively the two devices will, in general, give different results. Therefore, while this document compares and contrasts FWD- and TSD-based indices, the reader is advised to focus on trends and not the magnitudes (furthermore, the time difference between the two sets of FWD and TSD measurements is more than 7 years). An important consequence of the two devices not giving the same quantitative values is that thresholds based on FWD-derived indices are not directly applicable to TSD-derived indices. The fact that the TSD does not give the same quantitative results as the FWD does not mean either device is not accurate. The accuracy of the TSD has been investigated by Rada et al. (2016), who validated TSD measurements with "ground truth" measurements performed on instrumented pavements.

In addition to SCI300, there are a large number of deflection-basin related indices that have been proposed by researchers; listing these indices is beyond the scope of this report. The interested reader is referred to Table 44 of Rada et al. (2016), where 75 indices, which were evaluated in that study, are listed. Although the number of indices is quite large, most are so highly correlated (some almost identical) that essentially only a small number of the indices are needed to meet the objectives of this effort. For this pooled fund study, the SCI300 and DSI, have been selected and reported. DSI, shown in Equation 4, was recommended by Rada et al. (2016), and is the difference between the deflection at 100 mm (4 in.) from the applied load and the deflection at 300 mm (12 in.) from the applied load.

$$DSI = D100 - D300 \quad (4)$$

The DSI and SCI300 were found to be correlated to the tensile strain at the bottom of the asphalt layer as follows:

$$\varepsilon = a(DSI)^b \qquad \varepsilon = a'(SCI\,300)^{b'} \quad (5)$$

where *a*, *b*, *a'*, and *b'* are parameters obtained by Rada et al. (2016) that depend on the thickness of the asphalt concrete layer.

Temperature Correction of TSD Measurements

Pavement temperature is an important parameter that affects the results of flexible pavement structural evaluations. The deflection indices computed from TSD measurements are a function of pavement temperature at the time of data collection. Consistent evaluation and tracking of the indices computed from TSD measurements over the pavement service life requires that the indices be adjusted to a standard reference temperature. Due to the TSD being a relatively new

device, currently there are no proven methods to correct TSD measurements for temperature. However, Rada et al. (2016) have proposed a method to correct the tensile strain at the bottom of the asphalt layer. The approach is based on the change of the asphalt concrete (dynamic) modulus, which affects the tensile strain at the bottom of the asphalt layer. The steps for this procedure are (from Rada et al. 2016):

1. Compute the asphalt layer dynamic modulus at the test temperature, E_f, based on the calculated strain (from DSI or SCI300 using Equation 5) using the following equation:
$$E_f = c \times \varepsilon^d \quad (6)$$
where c and d, are model parameters that depend on the asphalt layer thickness. When the thickness is not known, default values are provided.
2. Compute a temperature correction factor, T_c, for the dynamic modulus as follows:
$$T_c = 19.791\left(e^{-0.043T_r} - e^{-0.043T_f}\right) \quad (7)$$
where T_r is the reference temperature (typically 70°F) and T_f is the asphalt temperature during the test.
3. Compute the dynamic modulus, E_r, at the selected reference temperature as follows:
$$E_r = \frac{E_f}{1 - T_c} \quad (8)$$
4. Compute the strain, ε_r, at the selected reference temperature by rearranging Equation 6 as follows:
$$\varepsilon_r = \left(\frac{E_f}{c}\right)^{\frac{1}{d}} \quad (9)$$
5. Calculate the temperature corrected TSD index using the inverse of Equation 5.

The asphalt temperature, T_f is taken as the mid-depth temperature and calculated from the measured surface temperature using the Bells equation (BELLS3):

$$T_f = 0.95 + 0.892 * IR + \{\log(d) - 1.25\}\{-0.448 * IR + 0.621 * (1\text{-day}) + 1.83 * \sin(hr18 - 15.5)\} + 0.042 * IR * \sin(hr18 - 13.5) \quad (10)$$

Where:
T_f = Pavement temperature at mid-depth d, °C
IR = Pavement surface temperature, °C
log = Base 10 logarithm
d = mid-depth of the AC layer, mm
1-day = Average air temperature the day before testing, °C
sin = Sine function on an 18-hr clock system, with 2π radians equal to one 18-hr cycle
hr18 = Time of day, in a 24-hr clock system, but calculated using an 18-hr asphalt concrete (AC) temperature rise-and-fall time cycle

Greenwood Engineering reports GPS location and time at each interval (10m) in the file ending with ".gpsimp.xls". Note GPS time is presented in Coordinated Universal Time, UTC. Pavement surface temperature is also reported along with the deflection values in the file ending with "tsd.tsd.xls". The previous day average air temperature was obtained at the closest weather station from National Center for Environmental Information weather site https://gis.ncdc.noaa.gov and used in Bells equation to calculate mid-depth temperature. The computed mid-depth temperature is used with the temperature correction procedure described earlier. The following points should be noted when the results from temperature correction and repeatability analysis are evaluated.

1. Temperature correction procedure should be considered as an intermediate solution until an accurate procedure is developed.
2. Pavement layer details were available for only interstate routes, and were not readily available for other tested sections and therefore, for the purpose of temperature corrections, all sections were assumed to be flexible pavements. Consequently, the temperature corrected SCI300 should only be used for those pavement sections that Virginia DOT knows to be flexible pavements. For sections that are not flexible pavements, it is recommended to use the uncorrected SCI300 or other indices presented.
3. For roads where the AC layer thickness was not provided by Virginia DOT, default thickness was assumed based on the road category.
4. M&R activities, if any, applied between the time of initial and repeat data collection are not considered in the repeatability analysis.

RESEARCH QUESTION 2: WHAT IS THE STRUCTURAL CONDITION OF THE TESTED ROADS?

The tested roads included interstates, primary roads, and secondary roads. The interstate roads tested comprised 72 miles of I-81 South from milepost 222 (I-64 exits) to 150 (exit 150), 43 miles of I-95 North from milepost 11 to milepost 54, and 31 miles I-64 West from milepost 118 (U.S. 29 exit) to milepost 88 (I-81 exit). The tested primary roads were U.S. 29 North (107 miles) and U.S. 29 South (54 miles), U.S. 460 East (47 miles) and U.S. 58 East (84 miles). Figure 3 shows the tested road sections. The secondary roads tested were off U.S. 29, U.S. 58, and I-95. Repeated measurements were performed on Route 29. Table 1 lists the roads tested with corresponding Google Maps© links. Clicking those links will show the corresponding tested road in a Web browser, as illustrated in Figure 4. In total 622 miles, including repeated sections, were tested over a period of 3 days (June 15 to 17, 2016).

Figure 3. TSD-tested roads shown in Google Earth.©

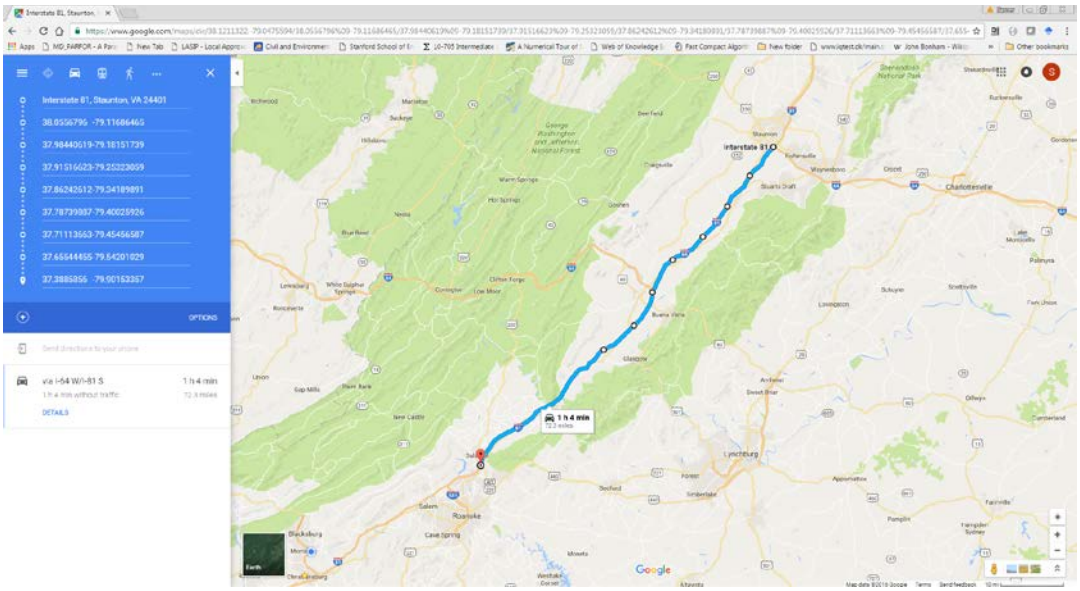

Figure 4. GoogleMaps© link showing tested route on I-81 South.

Table 1. TSD-Tested Roads with Test File Information and Google Maps Links

File	File Name	Roads	Length (miles)	Link
1	T7201506150001	US 29 North – I-64 West – I-81 South	166	https://goo.gl/maps/R93hY7RRM9R2
		US 29 North	62	https://goo.gl/maps/tBivd42p5er
		I-64 West	31	https://goo.gl/maps/J1QGpTEsFuv
		I-81 South	72	https://goo.gl/maps/5A6dFXbuhTL2
2	T7201506150002	US 220 AL- US 460	52	https://goo.gl/maps/SxhsuaVbsd22
3	T7201506150004	US 29 South	55	https://goo.gl/maps/G2mbgNqrwCU2
4	T7201506150006	SR 40– PS 685 (Passenger Route 685)	15	https://goo.gl/maps/cvjzCAA3G1R2
5	T7201506150007	US 29 North	46	https://goo.gl/maps/y3qMirXQaUn
6	T7201506160002	US 501 –US 29 South – SR 360	90	https://goo.gl/maps/rvZNJeYi1po
7	T7201506160004	US 58 – SR 664 – SR 660 –US 58	117	https://goo.gl/maps/3CrSYnwTTpP2
8	T7201506160005	I-95 North – SR 144 – US 301	45	https://goo.gl/maps/Lt2rPhMeP3v
9	T7201506170001	SR 629 – SR 156 – SR 616 – SR 666 – SR 609 – SR 636 – SR 635	22	https://goo.gl/maps/RVzDfKPfe5A2
10	T7201506170002	SR 635 – SR 618	7	https://goo.gl/maps/iVLHpA5EBy32
11	T7201506170003	SR 630 – SR 618 – SR 620 – SR 638	9	https://goo.gl/maps/ZStkQDWHaMx
12	T7201506170004	SR 636 – SR 631	5	https://goo.gl/maps/fsNsG16P4fM2

Overall Condition of Tested Roads

A methodology based on the number of remaining ESAL's was used to arrive at a preliminary estimate for threshold between good/fair and fair/poor segments. It is expected that the estimated threshold will be revised based on the experience gained from implementation effort.

Initially, three road category – Interstate, primary and secondary roads were considered based on AC layer thickness as shown in Table 2. The database generated in Rada et al. (2016) was used. The database contains a range of pavement structures (layer thickness) and material characteristics (layer moduli) values generated using Monte Carlo simulation and corresponding pavement responses (strain and deflections) computed using the layered linear elastic program JULEA. The pavement segments in the JULEA database was grouped in one of three road categories based on AC layer thickness as shown in the Table 2. In each pavement segment, number of repetitions to failure, N_f was computed using Asphalt Institute equation (Asphalt Institute. 1982))

$$N_f = C \times 0.00432 \left(\frac{1}{\varepsilon_t}\right)^{3.291} \left(\frac{1}{E}\right)^{0.854} \quad (11)$$

where C is the calibration coefficient, ε_t is the magnitude of the tensile strain repeatedly applied, and E is the stiffness of asphalt mixture (psi). The tensile strain at the bottom of AC layer corresponding to 9000 lb loaded dual tire configuration with 13.5 inch tire spacing and 116 psi tire pressure was used. The calibration factors that account for the effects of boundary difference between field and laboratory were 13.3 and 18.4 corresponding to the failure criteria of 10% and 45% of wheel-path cracking, respectively (Finn et al., 1977). C value of 13.3 was chosen for Interstate and Primary road category and 18.4 for secondary roads. In each road category the following level of annual traffic was considered

- Interstate: 1.4 million ESAL – equivalent of about 6500 ADTT (or 2000 singles, 4000 doubles and 500 trains or triples)
- Primary: 0.2 million ESAL – equivalent of about 950 ADTT (or 700 singles, 220 doubles and 30 trains or triples)
- Secondary: 0.07 million ESAL – equivalent of about 375 ADTT (or 300 singles, 75 doubles).

The pavement is considered as 'poor' or 'fair' condition when the computed N_f is lower than the traffic level the pavement can carry in the next 2 and 5 years, respectively in the corresponding road category. For example, an Interstate pavement segment will be considered 'poor' if the computed N_f is lower than 2.8 million ESAL's (annual traffic * 2 years). Similarly, a secondary road is considered as 'fair' condition if the computed N_f is lower than 0.35 million ESAL's (annual traffic * 5 years) but greater than 0.14 million ESAL's (annual traffic * 2 years). Average indices values were computed within each group and reported as threshold values in the table.

Note that the current threshold cracking % being used to calculate N_f with AI equation would be incremental (delta) cracking not total cracking. Thus when we consider the existing damage, a pavement segment identified as poor could have a fatigue cracking higher than that defined in the table at the end of 2 years.

Once thresholds have been established, the temperature corrected indices (SCI or DSI) can be directly used to categories the pavement segment as good/fair/poor. For example in a Primary road section, if the SCI computed from TSD measurement is 5.0 mil then the pavement segment will be categorized as 'Fair'.

Table 2. Thresholds for SCI300 (TSD) and DSI

Road Category	AC layer thickness, inch	Annual Traffic, million ESAL	Threshold for Fatigue Cracking at Wheelpath, %	Threshold for Poor			Threshold for Fair		
				N_f, million ESAL	SCI300, mil	DSI, mil	N_f, million ESAL	SCI300, mil	DSI, mil
Interstate	> 9	1.4	10	2.8	3.7	3.0	7.0	2.7	2.2
Primary	6 - 9	0.2	10	0.4	6.2	5.2	1.0	4.9	4.0
Secondary	3 - 6	0.07	45	0.14	9.7	7.7	0.35	7.3	5.8

Figure 5 shows the condition of the tested roads using this procedure. For the Interstate roads, the AC thickness was obtained from the Virginia Department of Transportation (VDOT) PMS, and the SCI300 (and DSI) were corrected to a reference temperature of 70°F. For primary and secondary roads, the AC thickness was assumed to be in the range of 6 to 9 and 3 to 6 inches, respectively. Figure 6 shows a closer look at two road conditions. Again, the conditions depicted in the figure are based on preliminary condition thresholds developed to illustrate the concept and should be adjusted to match agency specific thresholds.

Figure 7, Figure 8, and Figure 9 show the overall structural condition, as indicated by the temperature-corrected SCI300, for the Interstate, Primary, and Secondary roads, respectively. The line with in the box represents the median of the measurements, the blue box represents the 50-percent range (25 to 75 percent), and the black whiskers represent the 90-percent range (5 to 95 percent) of the collected data. Note that the vertical SCI300 scales in each figure are different, especially for the Secondary roads, which are generally significantly weaker than the Primary and Interstate roads.

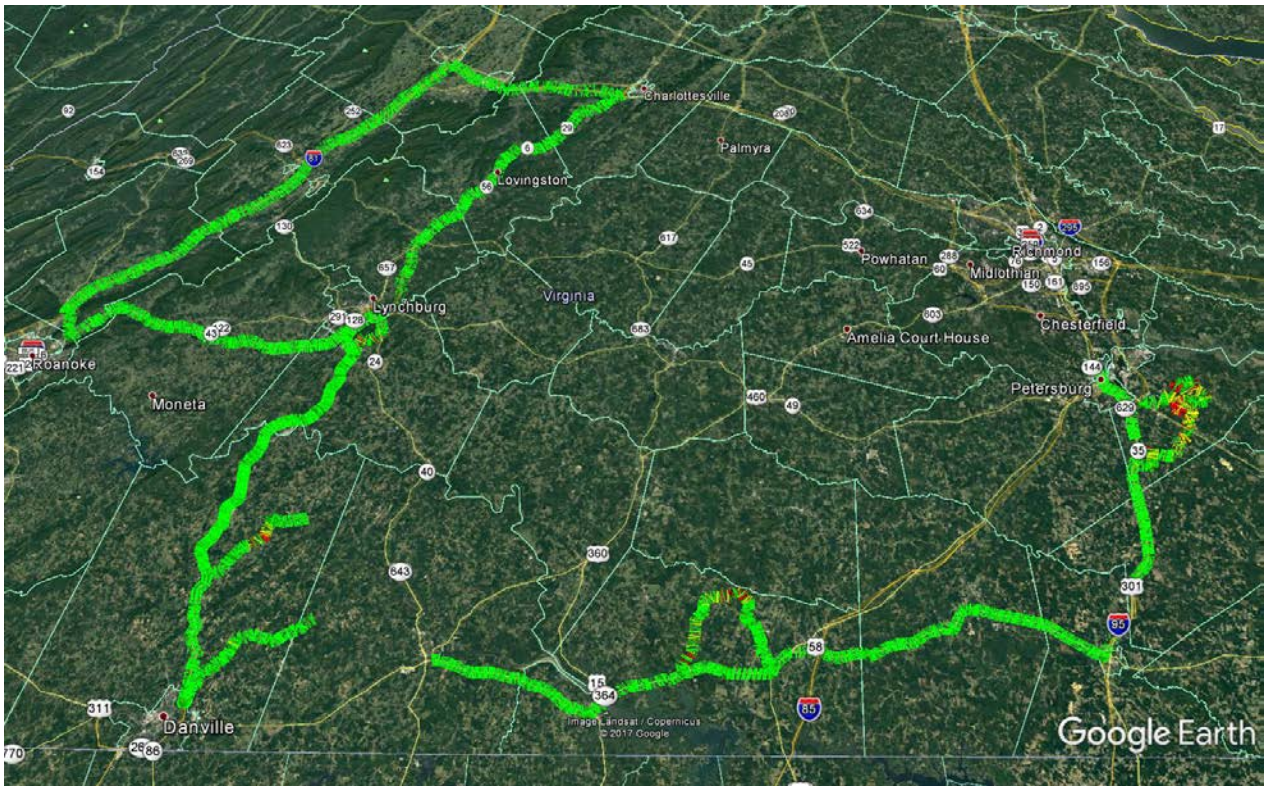

Figure 5. Color-coded condition of tested pavements with Good (green), Fair (yellow), and Poor (red) ratings (© 2016 Google Image Landsat / Copernicus).

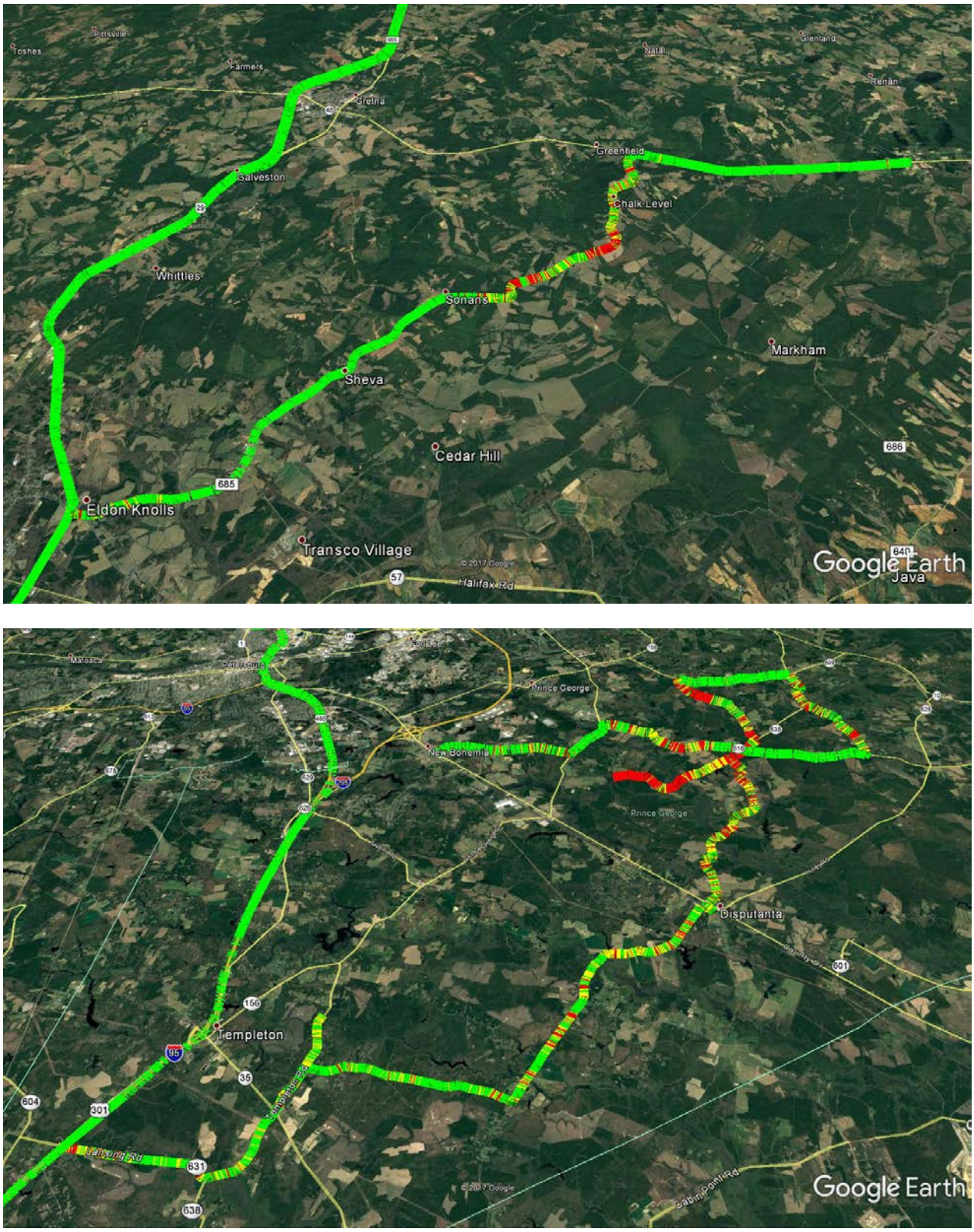

Figure 6. Two detail example of pavement condition (© 2016 Google).

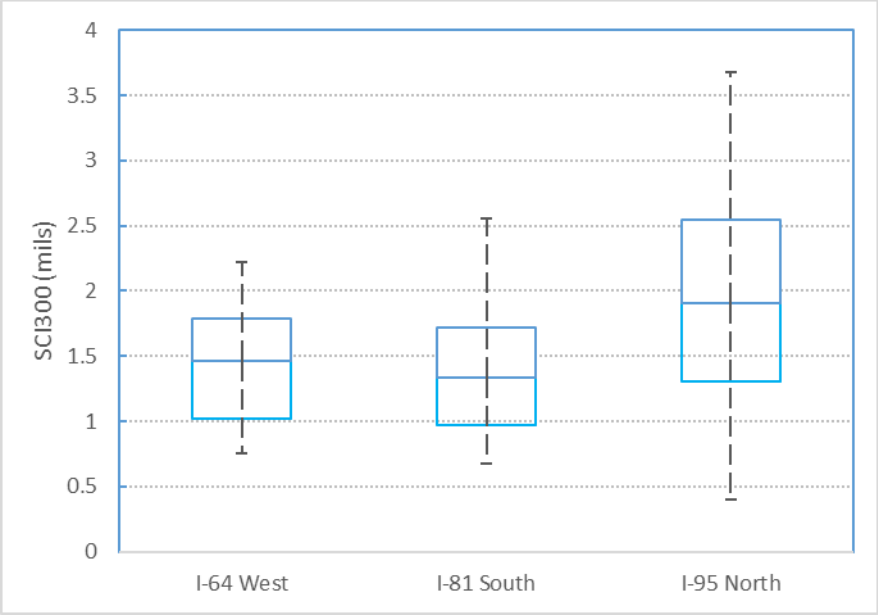

Figure 7. SCI300 box plot of Interstate routes.

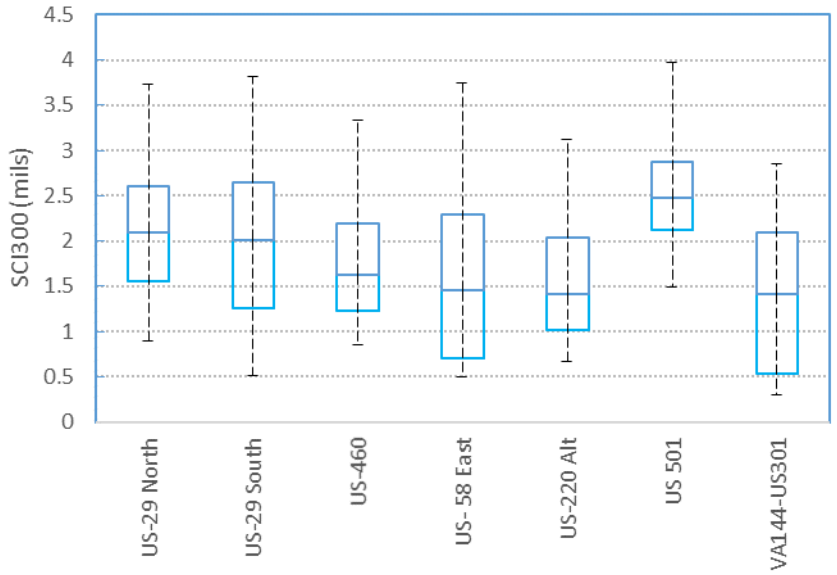

Figure 8. SCI300 box plot of Primary routes.

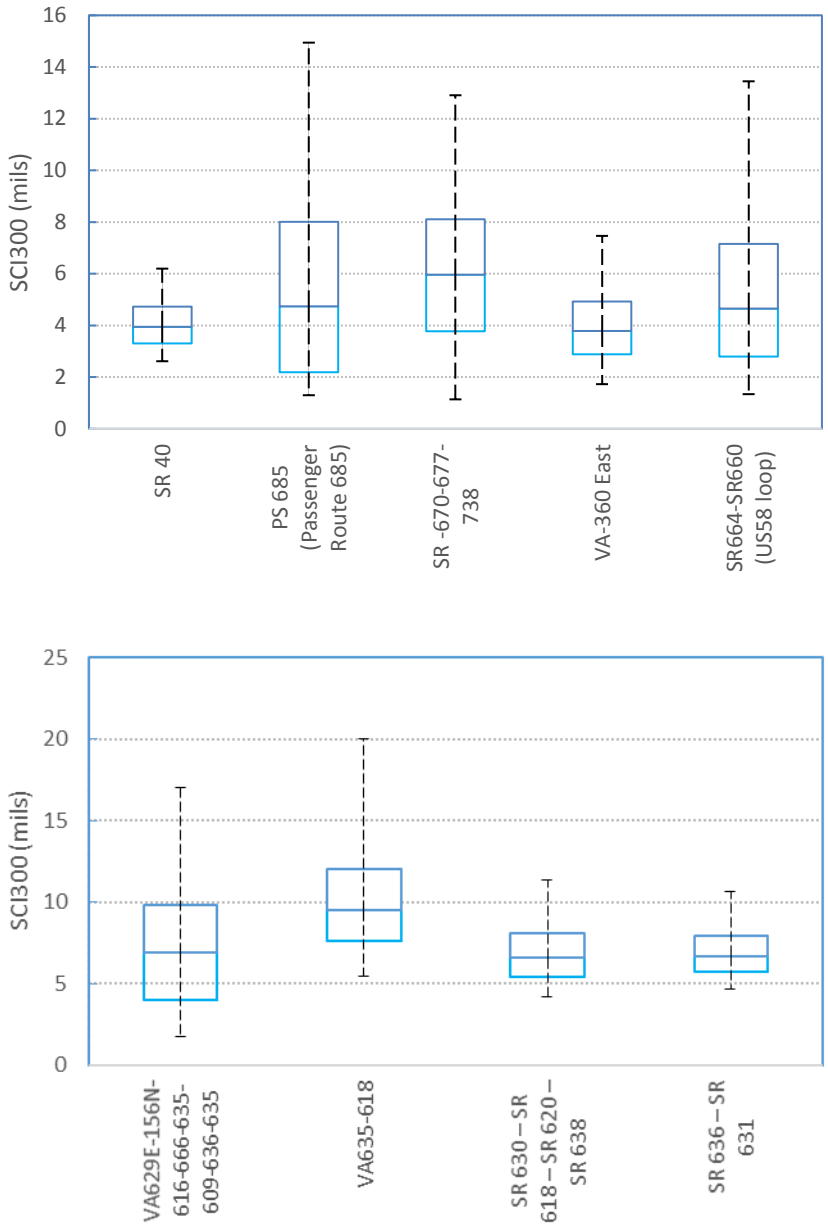

Figure 9. SCI300 box plot of Secondary routes.

RESEARCH QUESTION 3: HOW REPEATABLE ARE TSD MEASUREMENTS?

Repeated test runs were performed on two different days on U.S. Route 29 South from Lynchburg over a distance of 50 miles. The first run was performed on June 15, 2015; the second run was performed on June 16, 2015. Figure 10 shows the computed AC layer mid-depth temperature at the first day and the second day of testing. The temperature during the first day of testing was higher. Figure 11 shows the repeated runs corrected to the reference temperature of 70°F. The figure shows good repeatability over the length of the section. The sections that show minor

differences should be verified for the attribution of the factors stated in the section “Temperature Correction of TSD Measurements”.

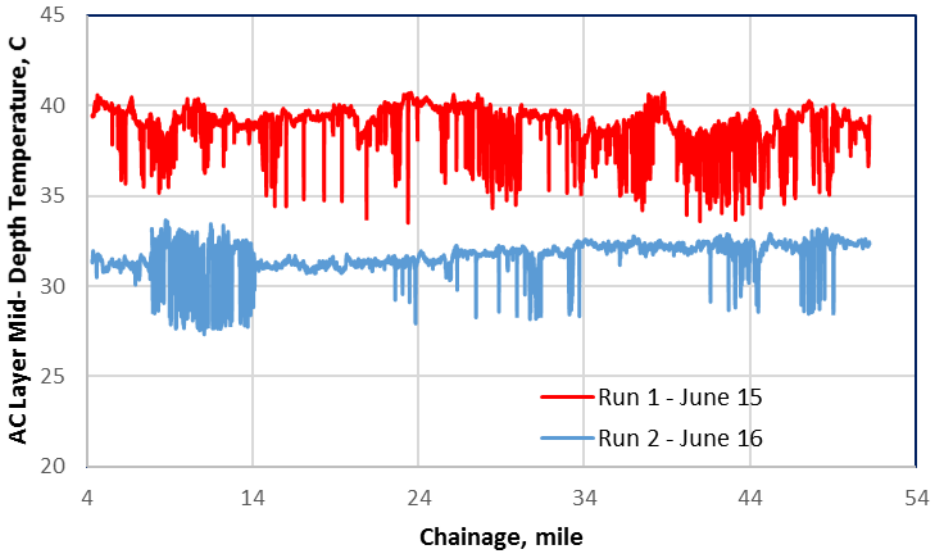

Figure 10. Mid-depth temperature between repeated tests in US 29 South.

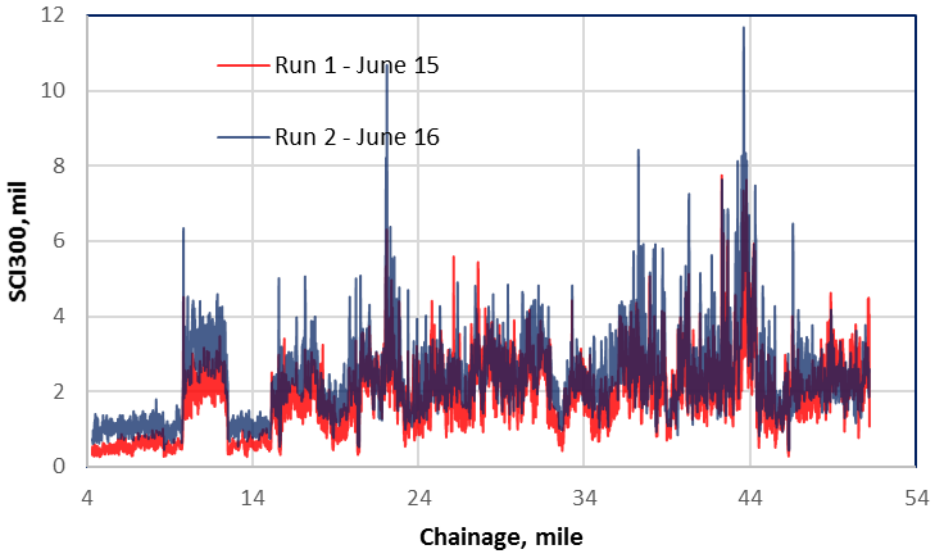

Figure 11. Repeated TSD tests on U.S. 29 South in Virginia performed on two consecutive days.

RESEARCH QUESTION 4: HOW DO TSD MEASUREMENTS COMPARE WITH FWD?

Test results from the TSD and FWD were compared. The comparison was based on the trends of TSD and FWD parameters, not specific values. Therefore, the TSD and FWD measurements shown have not been corrected for test temperature. Most of the FWD measurements were collected between 2006 and 2007. The TSD measurements were collected in 2015. This further justifies not performing a direct comparison between the two devices.

The FWD measurements were performed by VDOT on the interstate network between 2006 and 2007 at 0.2 miles intervals. These measurements were compared to TSD data collected in 2015 and averaged over a 0.1 mile length. In general, once heavy maintenance or reconstruction was accounted for, the results show that the FWD and TSD data followed similar trends, although not the exact same values (note that temperature correction was not performed). Figure 12 shows similar trends between D0 estimated from the TSD measurements and the FWD on I-81 South. However, the TSD estimated D0 are about 10 mil higher than the FWD D0 measurements. This discrepancy is expected and could be due to many factors, including different temperatures at the time of testing, differences in how deflections were calculated for the TSD, differences between how the two devices apply the load, and deterioration over the 8 to 9 years between the two tests. There are also some discrepancies between the two sets of measurements, mainly between mileposts 150 to 162 and particularly between mileposts 214 and 218. The section between mileposts 150 to 162 is a composite pavement section that underwent a series of rehabilitations, most notably jacking and grouting of the concrete slab in 2013 along with mill and overlay work that ranged from 3 to 5.5 inches. A possible hypothesis is that the weak spots measured by the FWD (high peaks observed in the plot) were strengthened by this series of rehabilitations, and thus these peaks are not observed in the TSD data. It is not possible to definitely confirm this hypothesis as no FWD data were collected after the pavement was rehabilitated.

The section between mileposts 214 and 218 was rehabilitated (using a variety of recycling methods) in 2011. Detailed structural information is available for this segment. Before the section was rehabilitated, FWD data were collected in 2010. After the rehabilitation was performed, FWD data were collected in 2011, 2012, and 2013. Details of the tested section are shown in Figure 13. The comparison of the FWD data between 2007 and 2010 shows that the structural condition of the section did not deteriorate in the 3- to 4-year period. (If any change is observed, the data suggest that the pavement slightly strengthened during that time period with the average temperature-corrected 2010 D0 being 10.86 mil and the average temperature-corrected 2007 D0 being 12.17 mil). The rehabilitation work improved the structural condition of the pavement section as reflected in the decreased D0 of FWD measurements performed in 2011, 2012, and 2013. The TSD-calculated D0 from the 2015 test follows the trend of the FWD results of 2011, 2012, and 2013, suggesting that the improved structural condition of the pavement section was also captured by the TSD measurements.

Further comparisons between the TSD and FWD measurements were performed with the calculated SCI300 on I-81 and D0 and SCI300 on I-95. Figure 14 shows the comparison of SCI300 computed from TSD and FWD on I-81, Figure 15 shows the results of D0 on I-95, and Figure 16 shows the results of SCI300 estimates on I-95. All the figures show TSD and FWD measurements following similar trends, although magnitude differs.

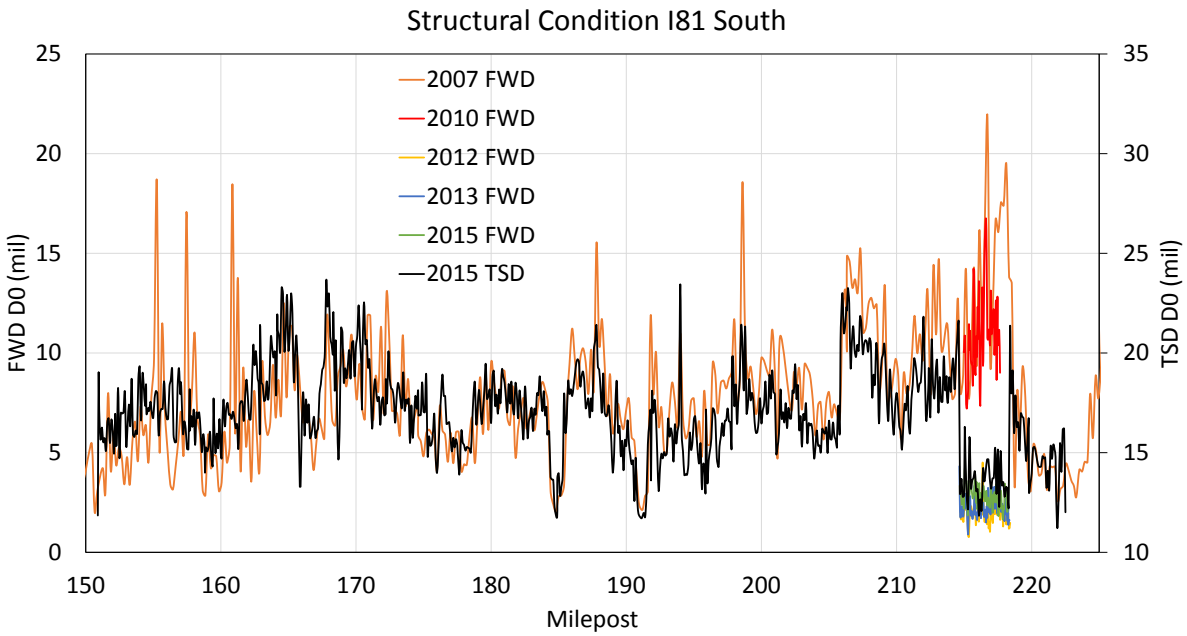

Figure 12. Comparison of TSD and FWD D0 on I-81 South.

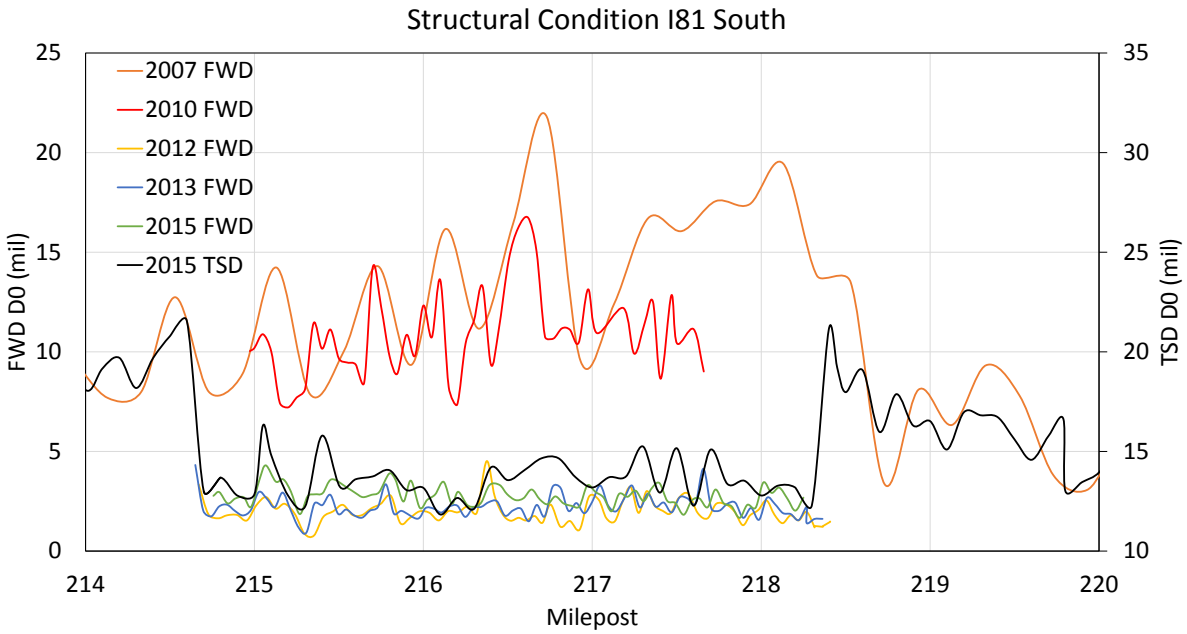

Figure 13. Details of comparison of TSD and FWD D0 on I-81 South.

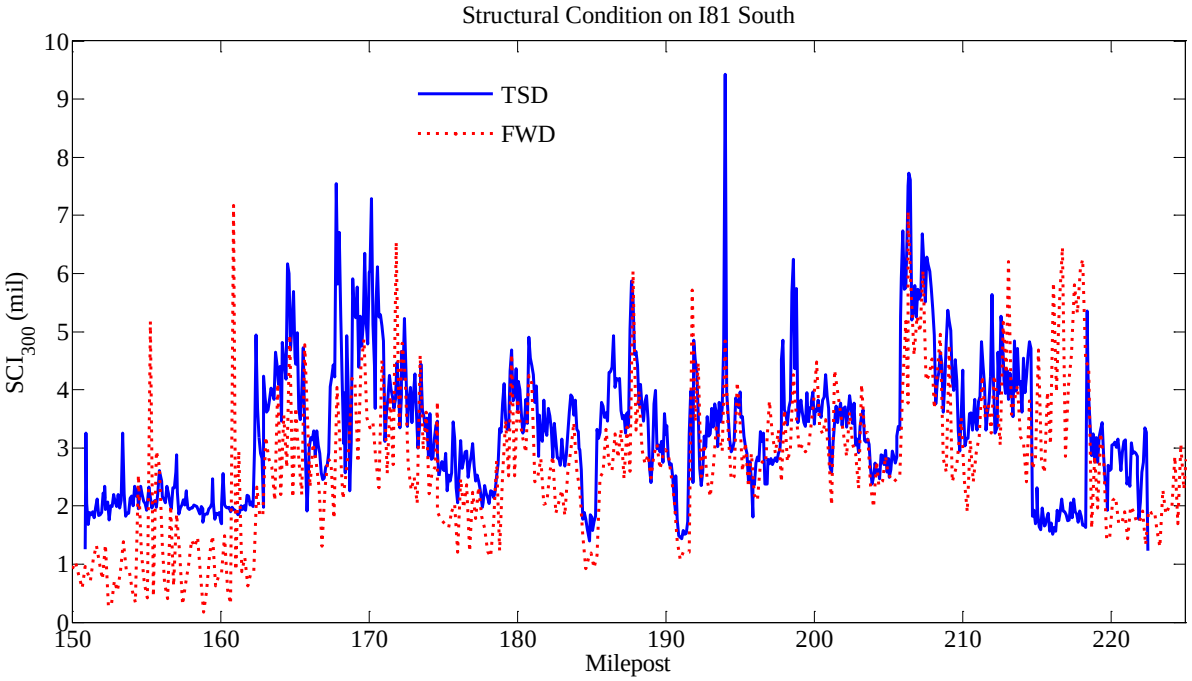

Figure 14. Comparison of TSD and FWD SCI300 on I-81 South.

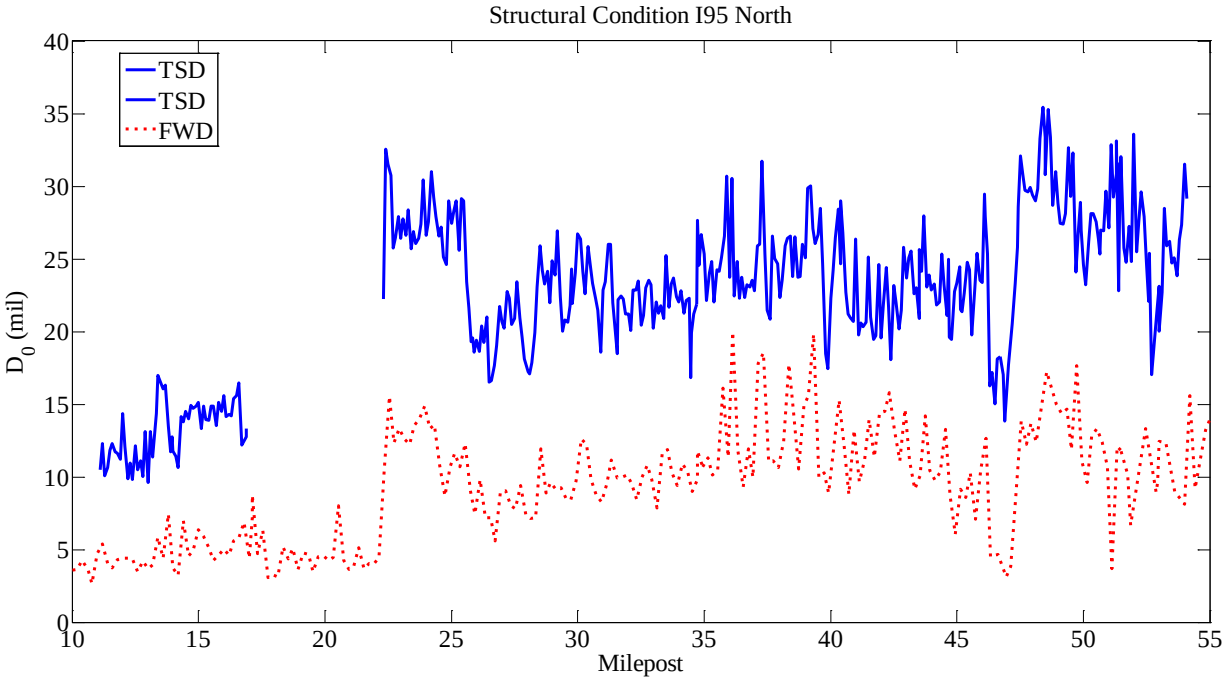

Figure 15. Comparison of TSD and FWD D0 on I-95 North.

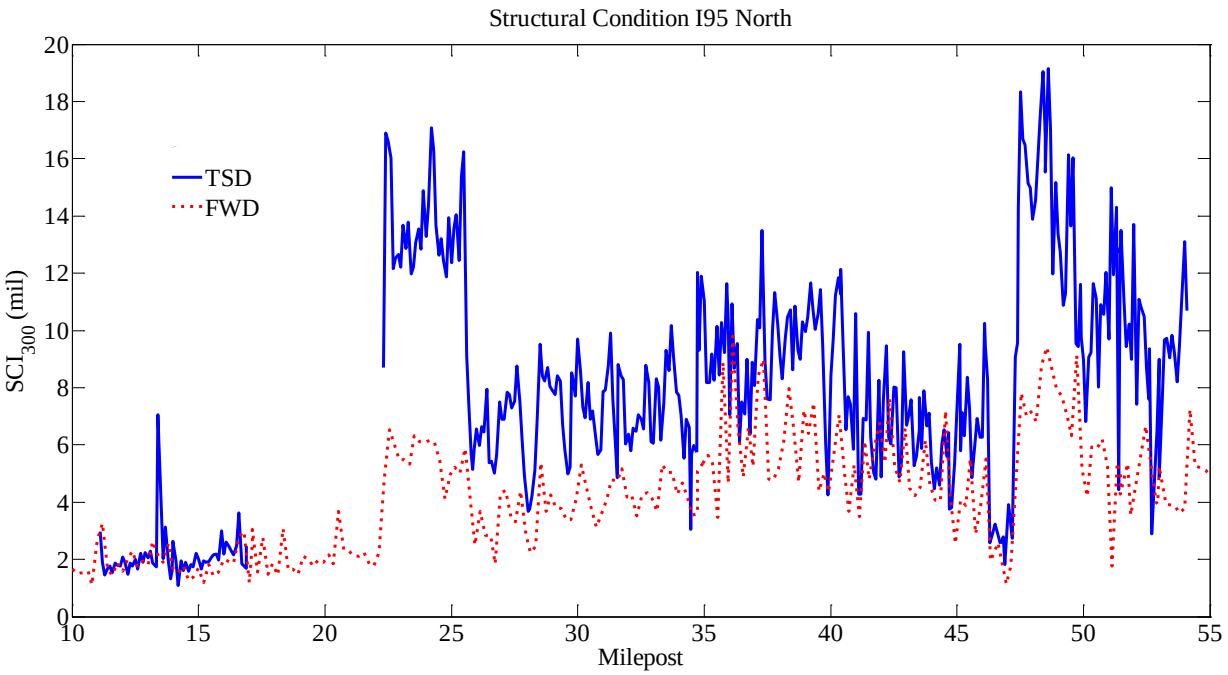

Figure 16. Comparison of TSD and FWD SCI300 on I-95 North.

Capability of TSD to Identify the Same Weak Sections as FWD

The capability of the TSD to identify the same weak sections as those identified by the FWD based on the calculated D0 was investigated. Because FWD measurements were collected every 0.2 miles, TSD measurements were averaged over a 0.2-mile length. Furthermore, sections that had a mill and overlay treatment or higher in the time between when the two sets of data were collected were not included in the analysis. The investigation was performed by determining the weakest 33%, 25%, 20%, 15%, 10%, and 5% of sections identified by each device and then determining in each case the percentage of sections that were identified by both devices. The percentages of commonly identified sections for each case were 70.5%, 67.1%, 60.3%, 60.4%, 56.5%, and 37.5%. Spearman's rank correlation, which is the correlation between the rankings of the all sections by each device, was calculated to be 0.816 (a Spearman's correlation of 1 means FWD and TSD give the exact same ranking of the sections).

To put these results into perspective, the same analysis was performed with two datasets from network-level FWD testing performed on I-81 in the Bristol district (a different location from where TSD testing was performed). The first FWD dataset was collected in 2006. The second dataset was collected in 2011 (note that the 5-year interval is smaller than the interval between FWD and TSD testing). Figure 17 shows the results of the testing, with the two datasets having similar trends. The percentages of sections that were identified as weak sections in both datasets were 58.6%, 56.6%, 52.2%, 48.0%, 45.5%, and 35.3% (from 33% to 5%). Spearman's rank correlation between the two datasets is 0.589. These results across all measures are not as good as those obtained with the TSD/FWD comparison. While the sections used for the two comparisons

were different, the comparison with the two FWD datasets shows that, even for the same device, identifying the same weak sections can be a challenging task. The performance of the TSD in identifying the same sections as those identified by the FWD from this small sample, then, is quite remarkable.

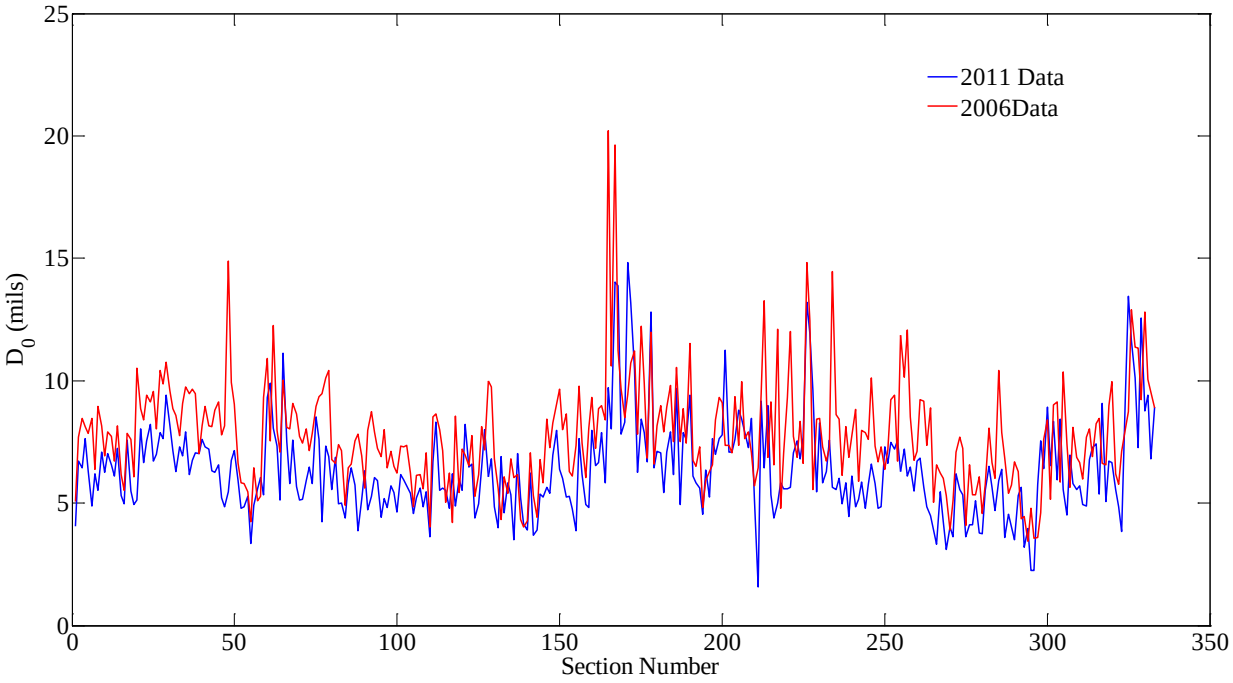

Figure 17. Comparison between two sets of FWD measurements on the interstate in the Bristol District.

RESEARCH QUESTION 5: HOW DO TSD MEASUREMENTS COMPARE WITH PMS DATA?

Pavement management data summarized at 0.1-mile intervals were obtained for the tested Interstate sections to compare with TSD test results. Figure 18 shows little correlation between SCI300 and Severity 1 fatigue cracking on I-81. Similarly, Figure 19 shows little relationship between SCI300 and a load-related distress rating index, LDR, used by VDOT to summarize the extent of all load-related distresses in an index that ranges between 100 (new "perfect" pavement) and 0 (failed pavement). Figure 20 shows the same for the Critical Condition Index, CCI, which combines load-related and non-load-related distresses in an index between 100 and 0. Figure 21 show the composite plot comparing SCI, categorized with the preliminary thresholds, with VDOT indices LDR, NDR and CCI. The estimated condition between the SCI and VDOT indices doesn't always agree - indicating the need for structural evaluation. Similar results of no relationship between PMS condition and SCI300 were obtained for I-64 and I-95.

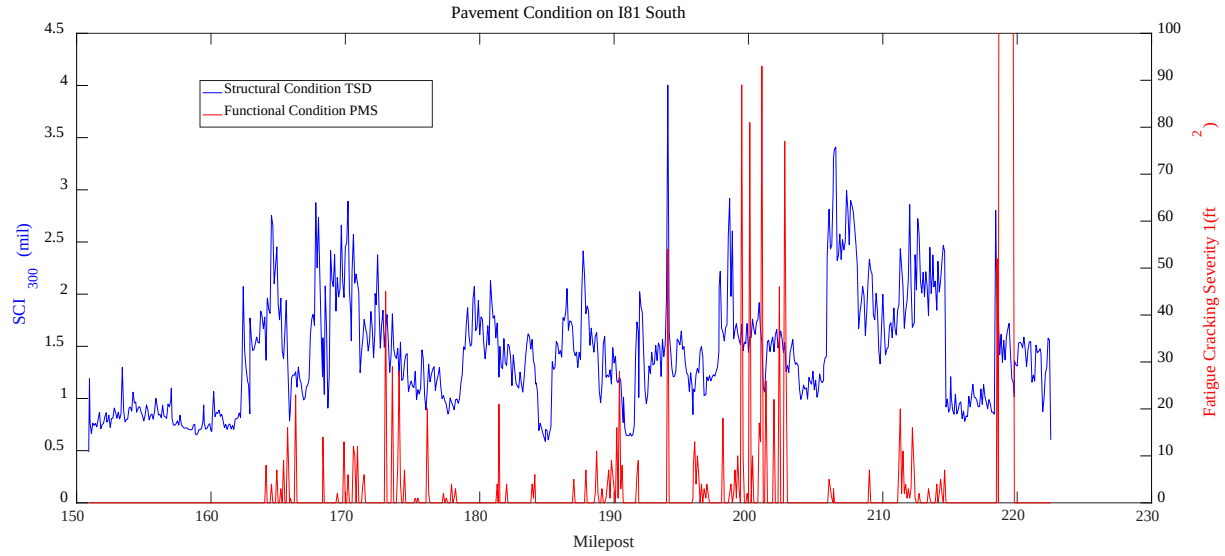

Figure 18. Comparison of TSD SCI300 and Severity 1 fatigue cracking on I-81 South.

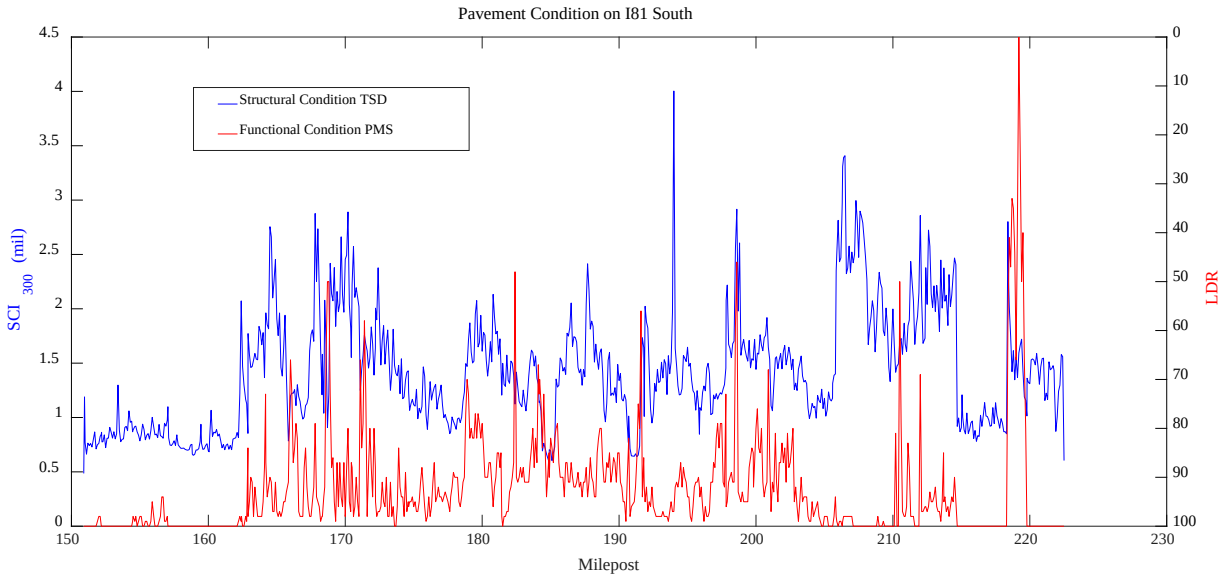

Figure 19. Comparison of TSD SCI300 and LDR on I-81 South.

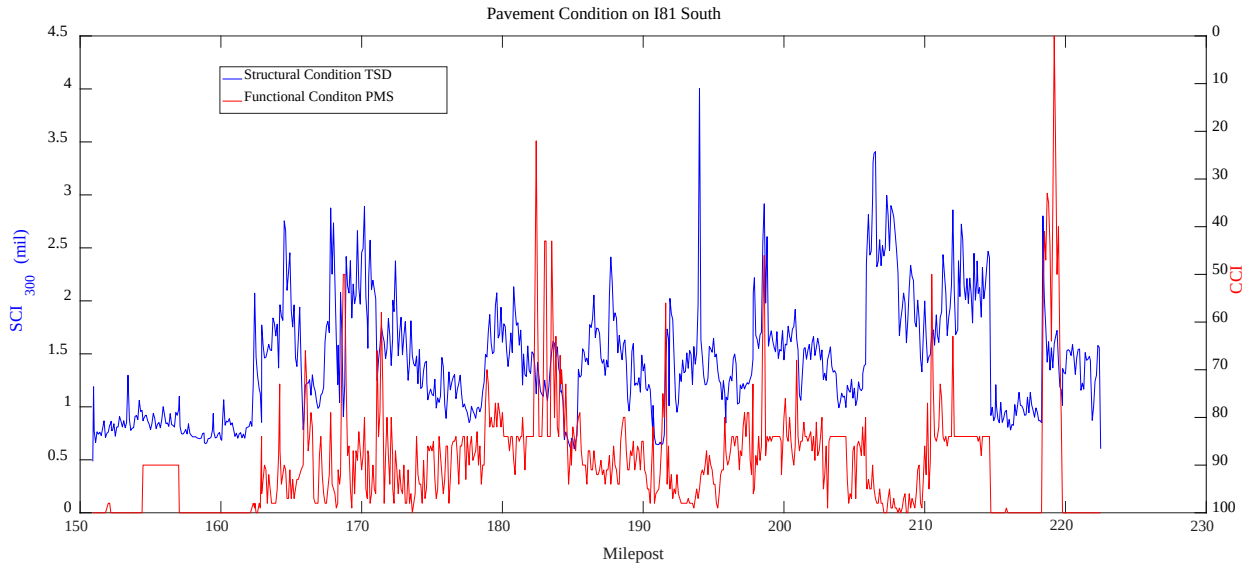

Figure 20. Comparison of TSD SCI300 and CCI on I-81 South.

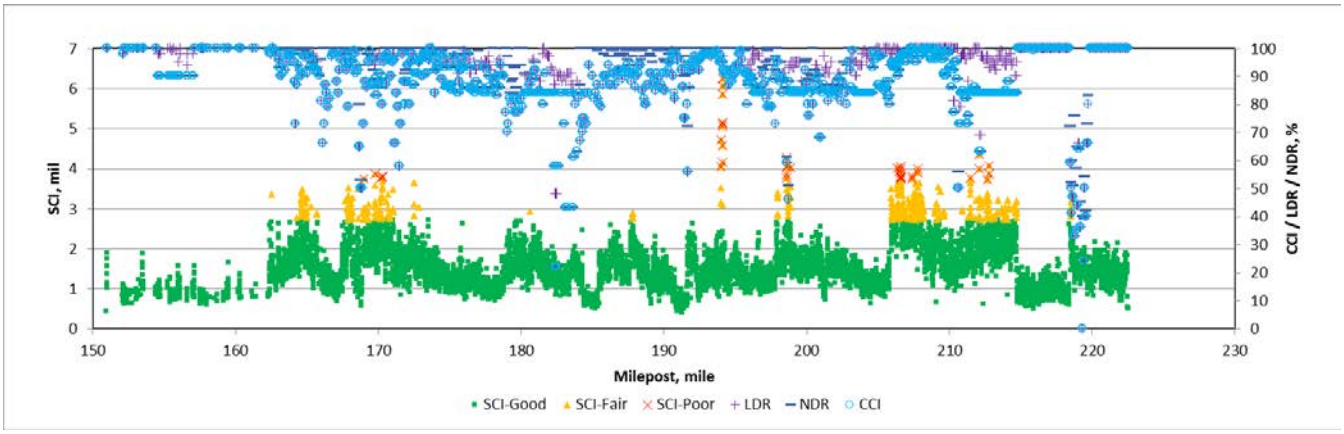

Figure 21. Strip chart for I81-South comparing SCI and three indices- LDR, NDR and CCI as computed from the surface distress data

Most sections on I-81 had zero to little measured fatigue cracking – mostly Severity 1 (see Figure 18). The same observation was also made for I-64. However, a more significant number of sections on I-95 had non-zero measured fatigue cracking. Figure 22 shows the Severity 1 fatigue cracking for the three interstate roads. More than 90% of I-64 and I-81 sections had practically no fatigue cracking compared with 50% of I-95 sections. Figure 23 and Figure 24 reinforce the observation that in general sections on I-95 have more distresses (in terms of Severity 2 fatigue cracking and CCI). In terms of work performed, most of I-95 had received a 3- to 4.5-inch mill and overlay between 2011 and 2012, but fatigue cracking reappeared rather quickly. On the other hand, some sections on I-81 and I-64 had received a mill and overlay treatment and are still performing well in terms of fatigue cracking. Furthermore, I-81 sections that have not received a mill and overlay between 2007 and 2014 are still generally performing well in terms of fatigue

cracking. Figure 25 shows the distribution of temperature-corrected TSD SCI300 for the three roads. The I-95 distribution shows higher SCI300 values and as such a weaker pavement. This sheds light on why more cracking is observed on I-95. Although a large portion of it has been recently resurfaced, these portions are still relatively weak, which is leading to fatigue cracking within a short time period. A subpopulation on I-95 has low SCI300 values, but this consists of a concrete pavement overlaid with asphalt and has practically no recorded cracking. Figure 26 shows the distribution of FWD SCI300 (collected between 2006 and 2007 and not temperature corrected) for I-81 and I-95, which also shows that I-95 has in general higher SCI300 values.

In terms of asphalt layer thickness, I-95 had an average thickness of 9.0 inches with a standard deviation of 1.25 inches. I-81 had an average thickness of 11.4 inches with a standard deviation of 1.38 inches. The ADTT on I-95 was 2,305 with a standard deviation of 295 and a maximum and minimum of 1,624 and 3,455. The ADTT on I-81 was 5,979 with a standard deviation of 804 and a maximum and minimum of 5,090 and 9,287. The Spearman rank correlation between SCI300 and Severity 1 fatigue cracking was 0.20 for I-81, 0.16 for I-95, and 0.40 for both combined. If composite pavement sections are excluded, the Spearman rank correlation for I-81 is 0 (all sections had 0% cracking), for I-95 is −0.02, and 0.42 for both combined. These results suggest that, in general, weaker pavement sections will exhibit more cracking (I-95 weaker than I-81); however, this is a very broad trend and observed cracking cannot be a substitute for pavement structural condition measurements (within each interstate, cracking does not correlate well with structural condition especially if only flexible pavement sections are considered). Two possible reasons are that the surface measurements do not show bottom-up fatigue cracks until they appear on the surface and the Severity 1 cracks might include top-down cracks that do not account for structural deterioration.

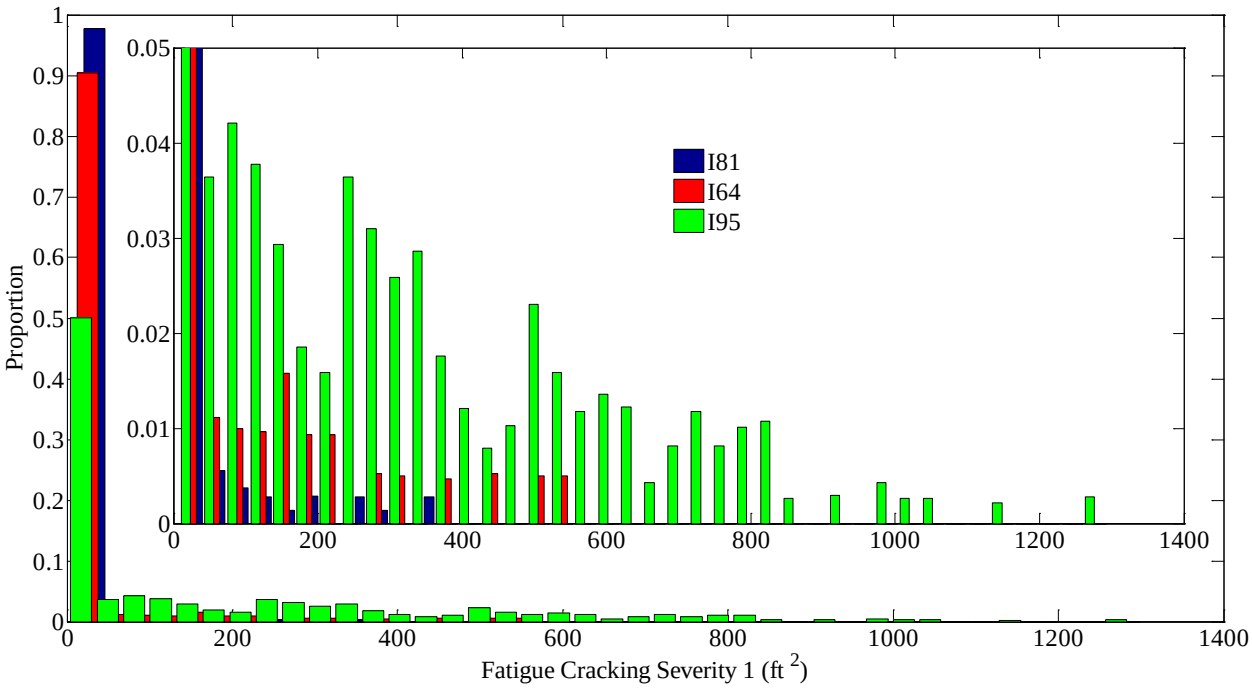

Figure 22. Observed frequency of Severity 1 fatigue cracking on tested Interstate sections.

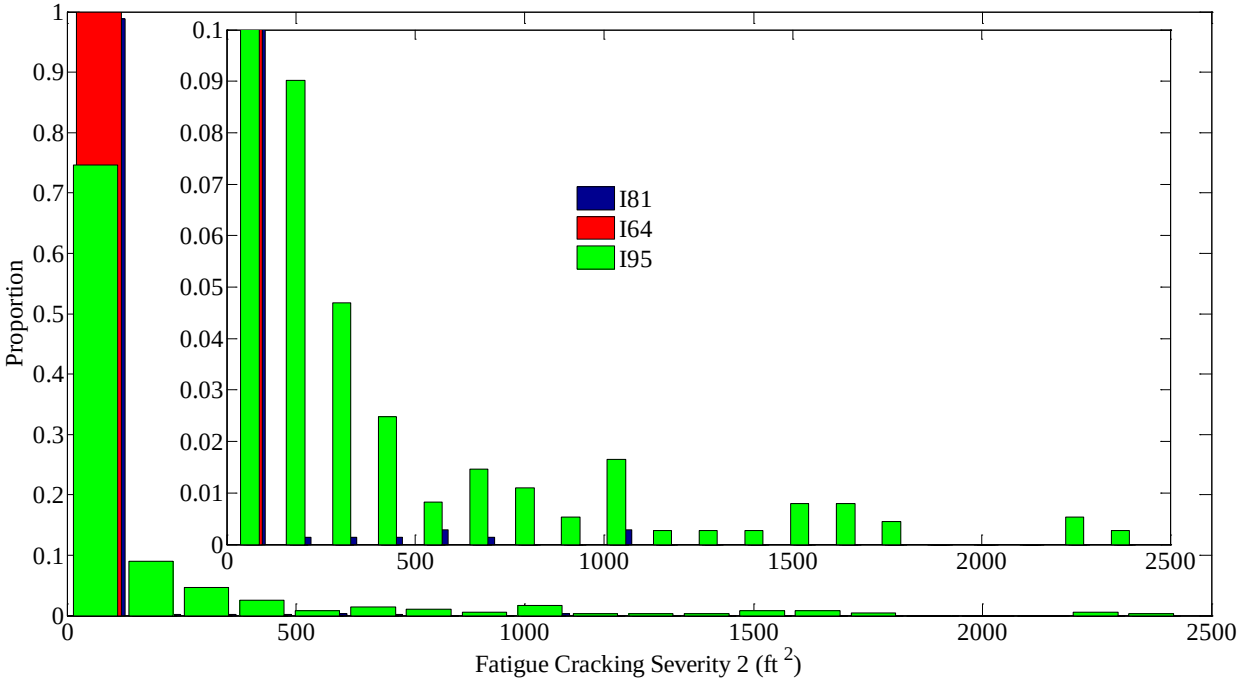

Figure 23. Observed frequency of Severity 2 fatigue cracking on tested Interstate sections.

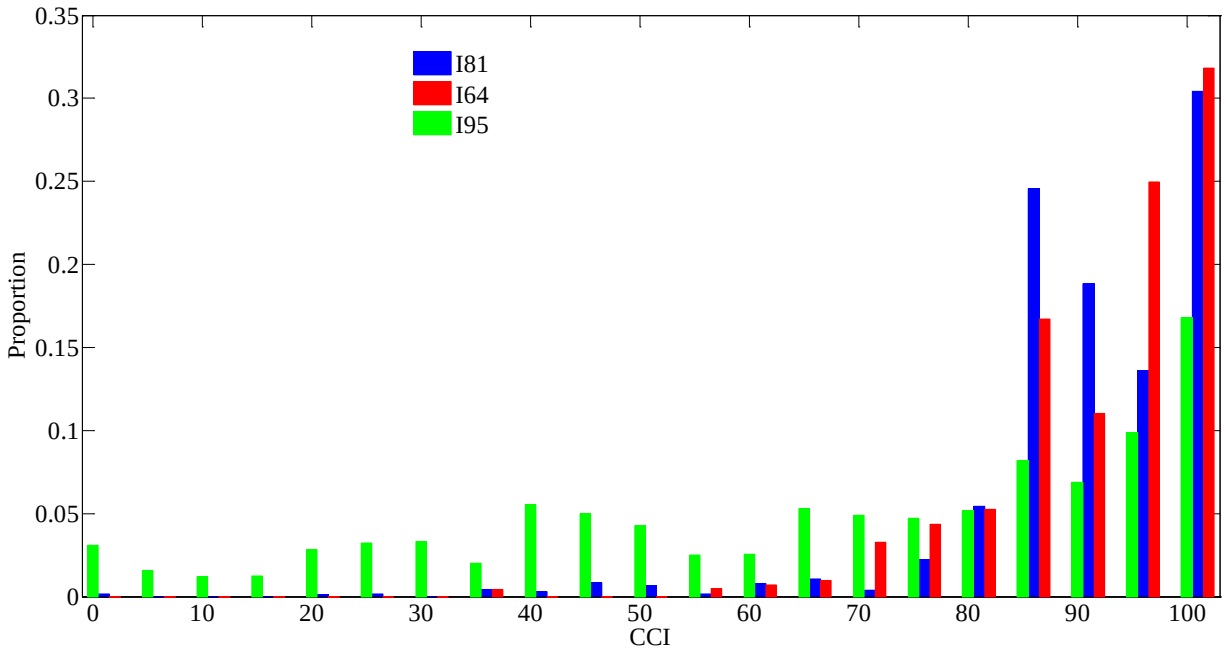

Figure 24. Observed frequency of CCI on tested Interstate sections.

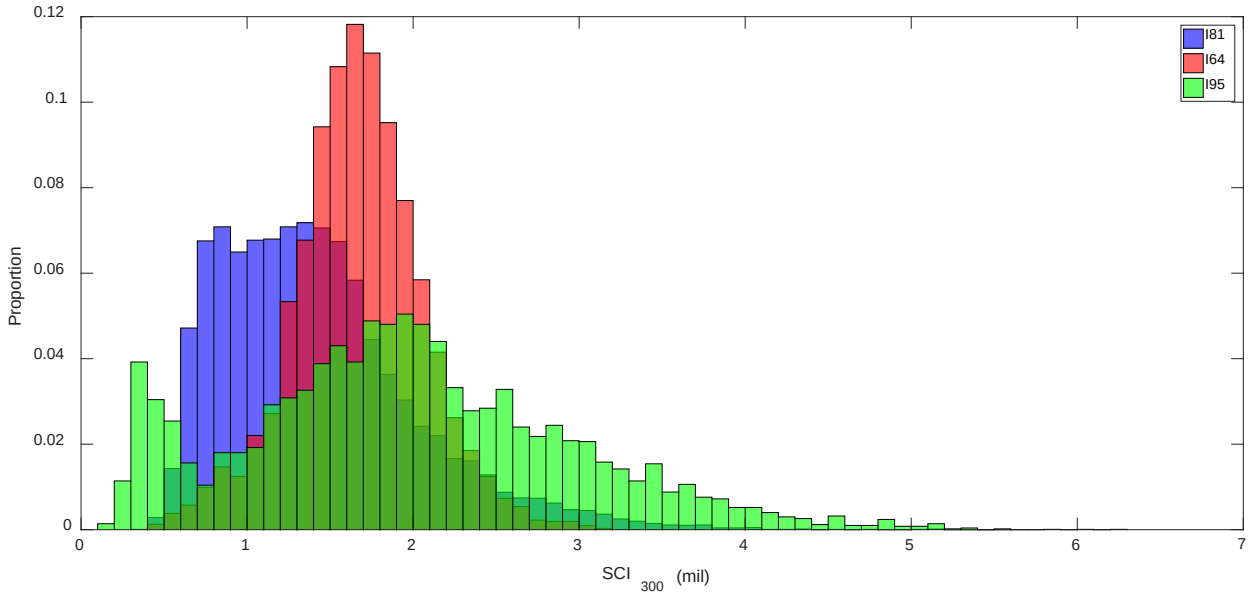

Figure 25. Observed frequency of TSD SCI300 on tested Interstate sections.

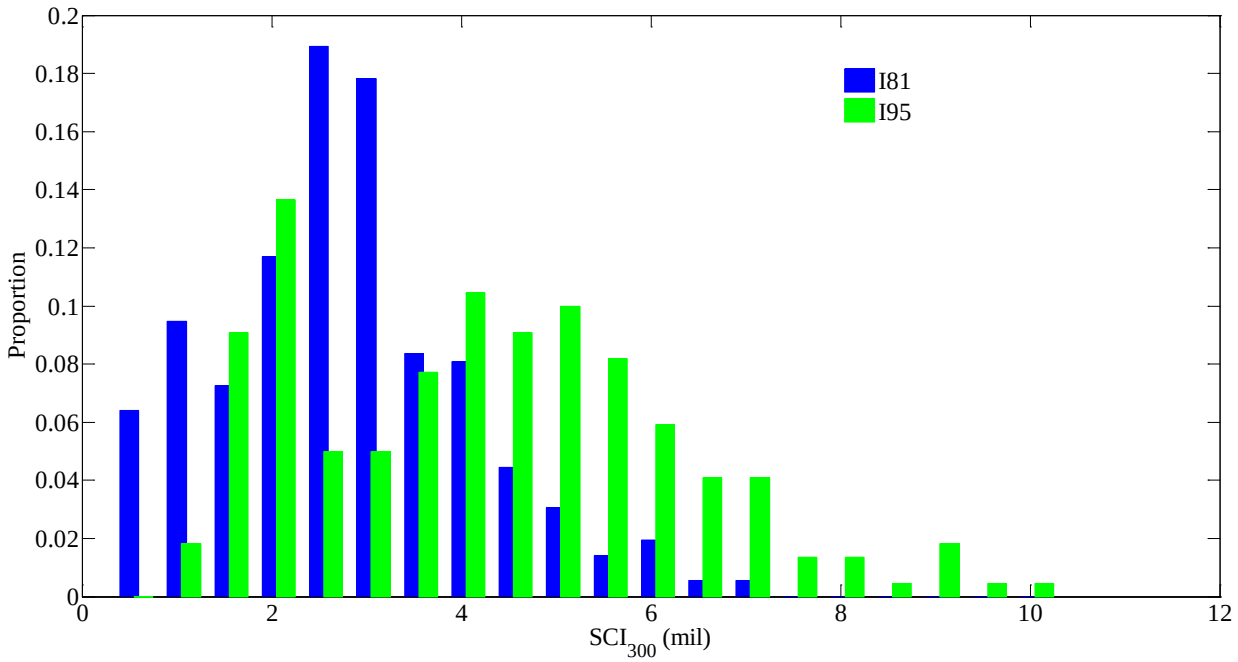

Figure 26. Observed frequency of FWD SCI300 on I-81 and I-95 sections.

Figure 27 shows the TSD calculated SN_{eff} for the I81-South. The SN_{eff} takes into account the pavement deflection as well as the pavement thickness. The calculation of the TSD SN_{eff} is performed using the method of Rohde (1994) as follows:

1. Determine the structural index *SIP* of the pavement as follows;

   $$SIP = d(0) - d(1.5H_P)$$

   where:
   $d(0)$ = peak deflection under the 9,000 lb load
   $d(1.5H_p)$ = deflection at lateral distance of 1.5 times the pavement depth.
   H_p = Pavement depth – thickness of all layers above the subgrade.

2. Determine the existing pavement SN_{eff} as;

   $$SN_{eff} = k_1 SIP^{k_2} H_p^{k_3}$$

   where for asphalt pavements, k_1 = 0.4728, k_2 = -0.4810, k_3 = 0.7581
   d(0) is temperature corrected to 68°F using the procedure stated in AASHTO 1993 guide. (AASHTO 1993)

Figure 27 also includes SN_{eff} computed using default layer coefficients as suggested in AASHTO 1993, which represents initial SN_{eff} of the pavement when constructed. The figure shows that the

TSD SN_{eff} is lower than the one estimated based on default layer coefficients indicating structural deterioration since initial construction. Also the structural deterioration is non-uniform over the pavement segment length. The figure also include LDR from the PMS for comparison. The condition estimation of TSD calculated SN_{eff} are found to be different from the LDR that were based on surface condition which shows the benefits of performing network level structural evaluation in better characterizing structural condition.

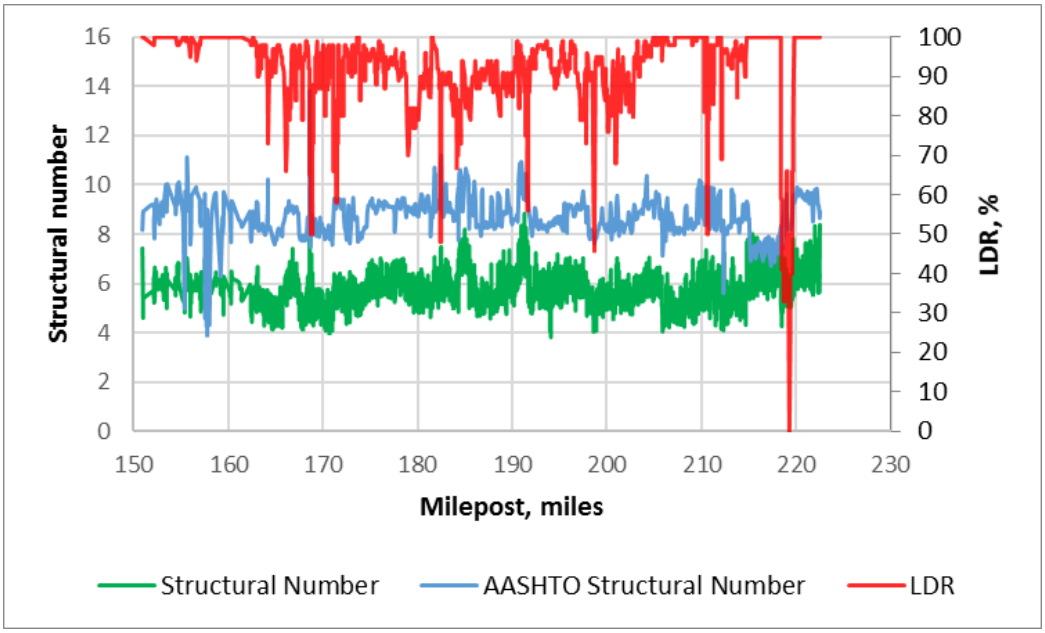

Figure 27. Comparison of TSD Structural number and LDR for I81- South

RESEARCH QUESTION 6: HOW CAN WE USE THE INFORMATION OBTAINED FROM TSD MEASUREMENTS?

In this section, we present examples on how TSD measurements can be used to help better manage pavement sections.

Identification of Strong and Weak Sections

TSD measurements can be used to classify pavement sections into structurally strong, fair, and weak categories (good, fair, and poor). Figure 28 shows an example of such a classification taken from part of the results presented in Figure 5. The classification could be used to determine where more detailed investigation of the pavement is needed. For example, identified weak sections could be assigned as candidate sections for heavier structural treatments; sections identified as fair could be assigned as candidates for lighter treatments, such as corrective or preventive maintenance or minor rehab based on surface distress measurements. The results presented in the

section on the comparison between the TSD and FWD suggest that, at least at the network level, the TSD will identify mostly the same weak sections identified by the FWD, with the difference between the two devices being similar to the difference in identification obtained with two different FWD datasets (note that this is not intended to suggest that it will also translate to project-level investigations at this stage).

Another validation of the capabilities of the TSD to classify sections is shown in Figure 29. Strong spots identified by the TSD along U.S. 29 south near Altavista are highlighted with the red circle. Upon further investigation, these spots were found to correspond to bridges, which in general are known to exhibit lower deflections than flexible pavement sections. The same was observed for most bridges on all tested roads.

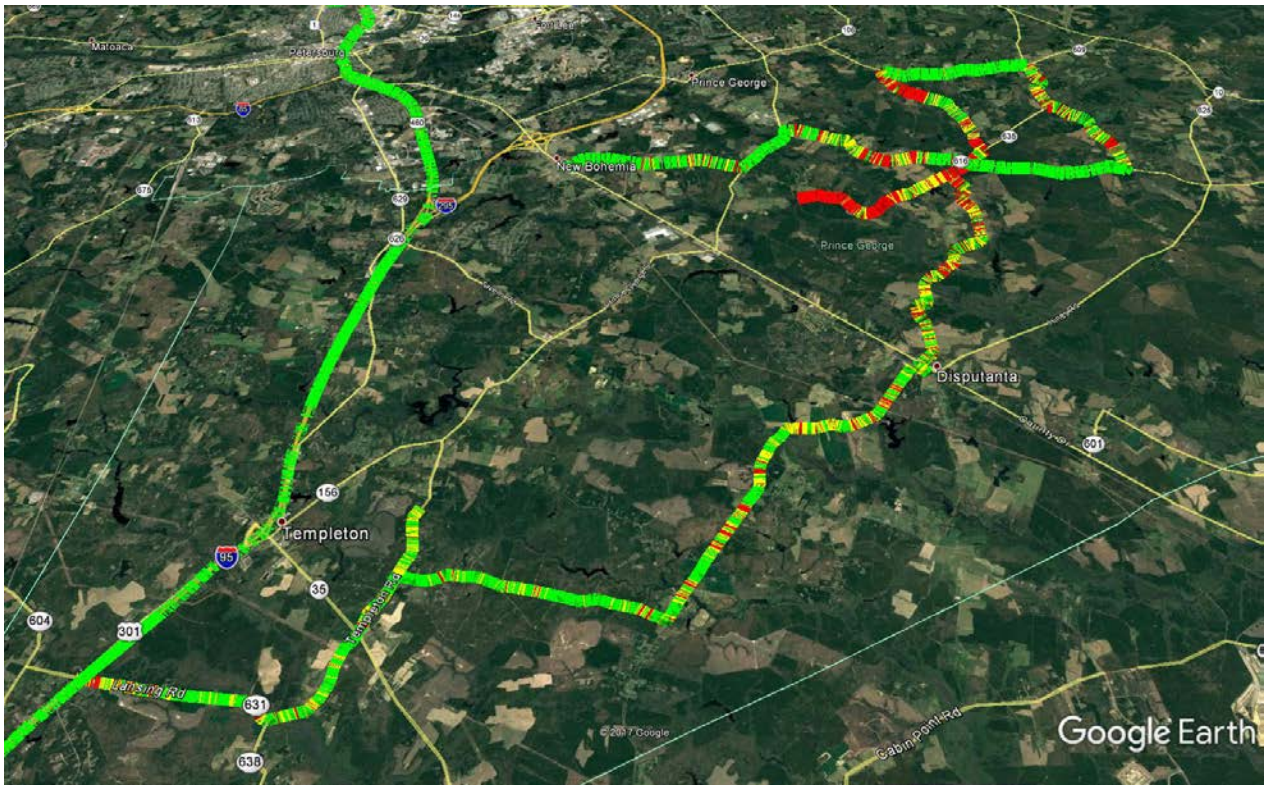

Figure 28. Identified Strong (green), Fair (yellow) and Weak (red) sections (© 2016 Google).

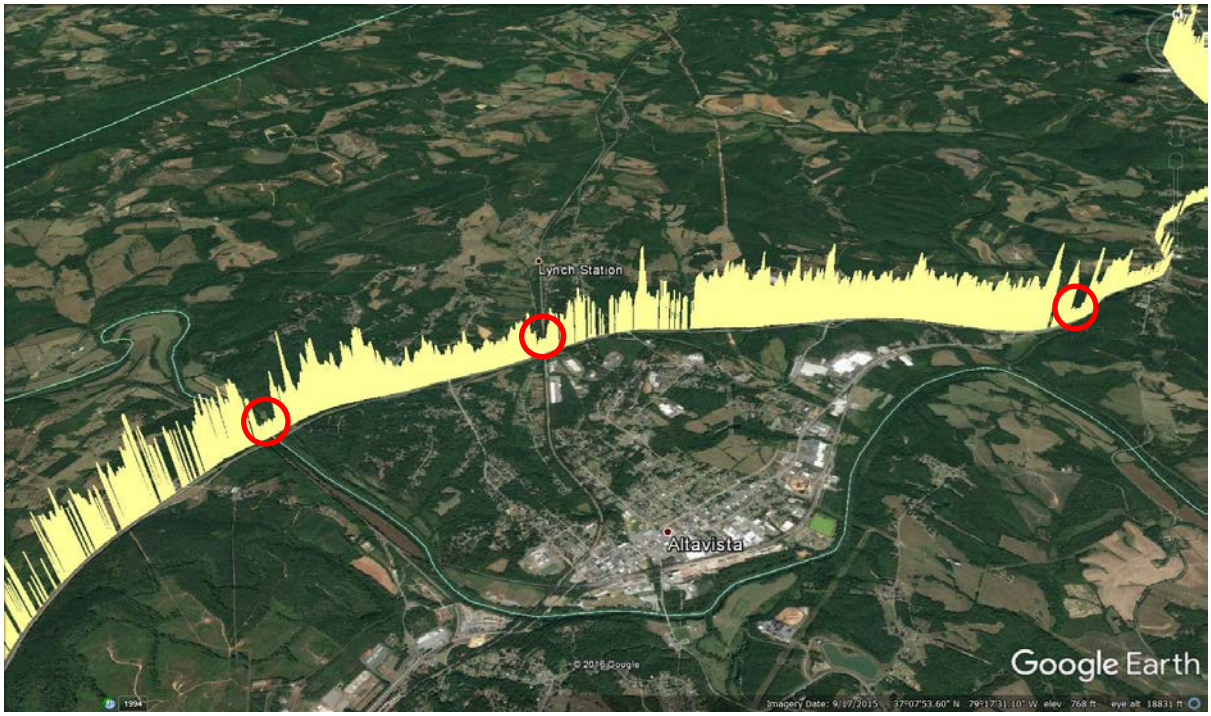

Figure 29. Identified Strong section corresponding to bridges on U.S. 29 (© 2016 Google).

Mechanistic Analysis with Asphalt Layer Tensile Strains

Work by Rada et al. (2016) has shown that the tensile strain at the bottom of the asphalt layer is highly correlated with pavement structural indices such as SCI300 or DSI that can be obtained from TSD measurements (see Equation 5 earlier). Figure 30 shows an example of the estimated tensile strain profile for I-95 (corrected to a reference temperature of 70°F). Thresholds of 100 and 150 microstrains, respectively, have been used to separate between good, fair, and poor structural conditions (these thresholds are arbitrary, the 100 microstrain was chosen since it was recommended for dynamic modulus testing of asphalt specimens to limit specimen damage). Again, the threshold should be based on the AC layer thickness and should be adjusted with experience. Figure 31 shows the strain before (average of 105°F) and after applying the temperature correction (to a reference temperature of 70°F) with corrected strains roughly 3.7 times smaller than uncorrected strains.

Another advantage of the strain approach is that it can be used with a locally calibrated fatigue life equation to provide a better estimate of the remaining fatigue life of the pavement section than the estimate obtained using the generic Equation 11. This provides a link between the TSD-measured condition with an estimate of the remaining structural life of the pavement as illustrated in Figure 32. Practical implementation of this procedure would be in the development of a structural index relationship with remaining fatigue life as illustrated in Figure 33 with the DSI.

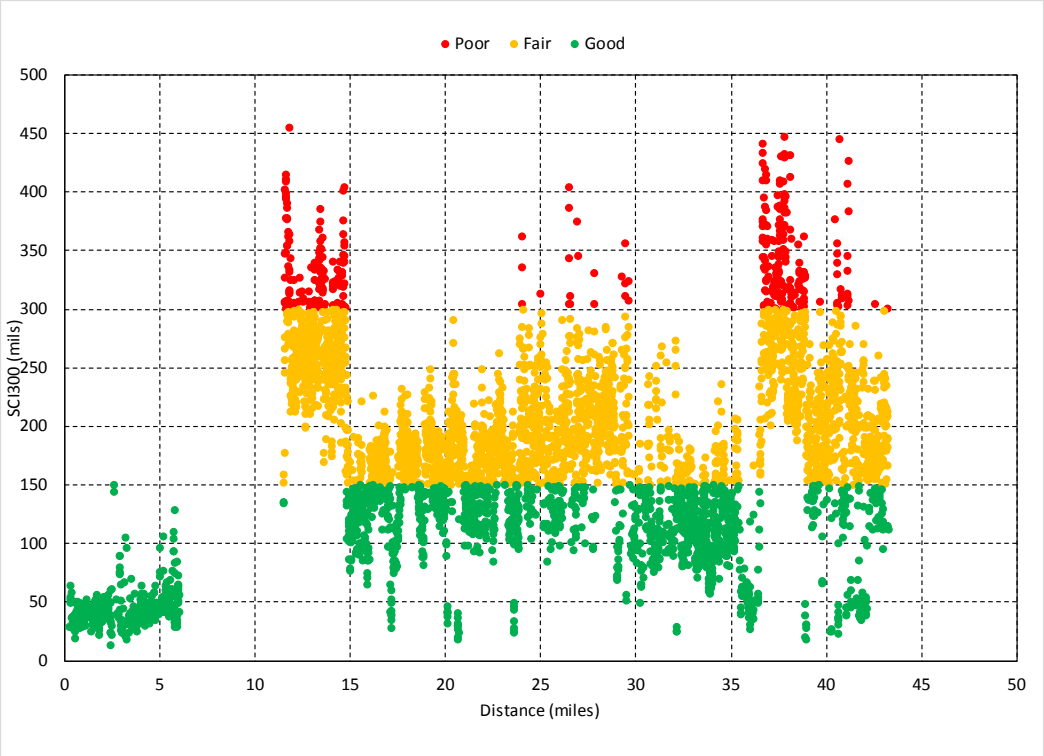

Figure 30. Estimated tensile strain at bottom of asphalt layer on I-95.

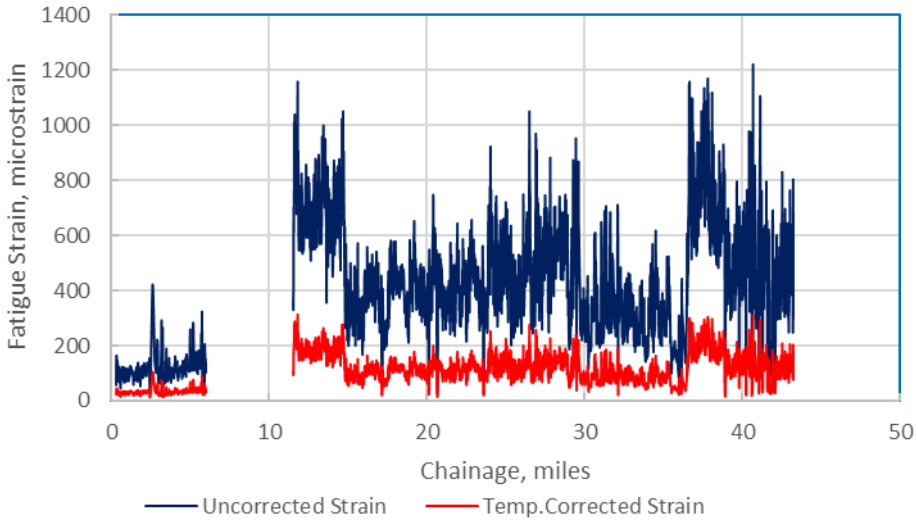

Figure 31. Estimated tensile strain at bottom of asphalt layer on I-95 showing effect of temperature correction.

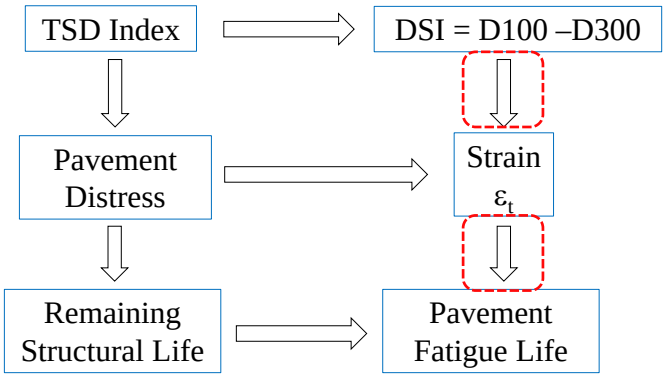

Figure 32. Link between DSI and estimated pavement fatigue life.

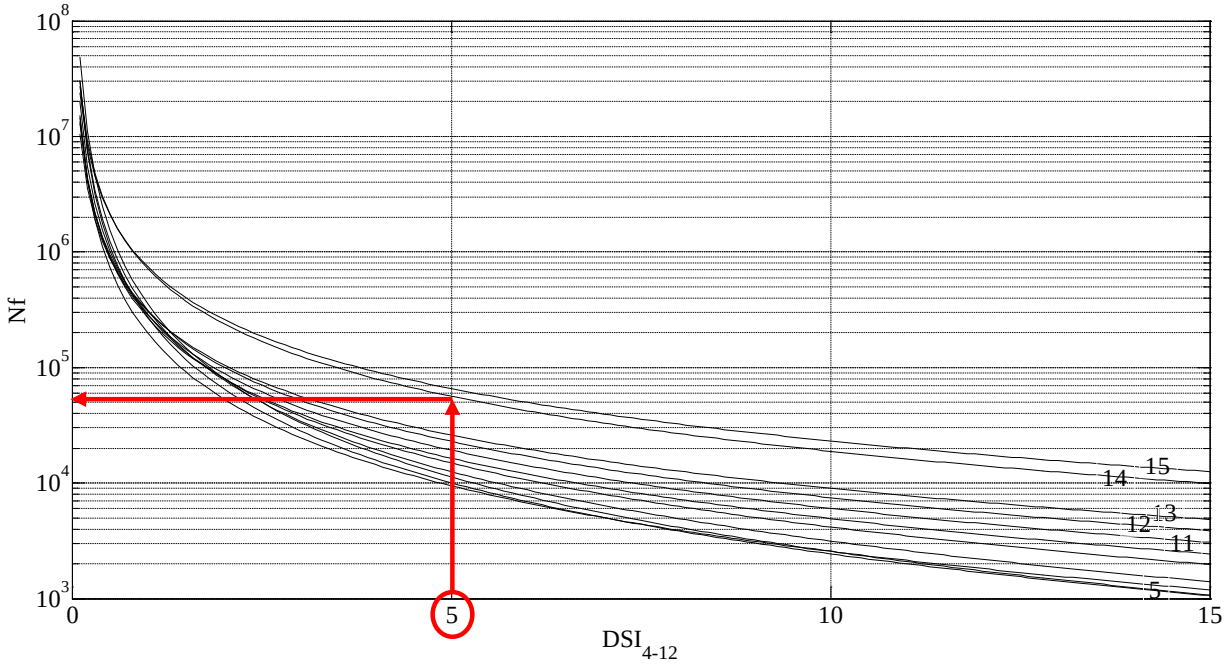

Figure 33. Fatigue life curves for TSD DSI.

RESEARCH QUESTION 7: HOW CAN WE INCORPORATE TSD MEASUREMENTS INTO A PMS?

VDOT uses a set of pavement management decision matrices with distresses as inputs and treatment activities as outputs. The matrices are separated based on the following roadway classifications: Interstates, Primary Routes, Secondary Routes, and Unpaved Roads, in addition to the following pavement types: bituminous-surfaced (BIT), bituminous-surfaced composite pavements (with jointed concrete pavement below the surface, BOJ), bituminous-surfaced composite pavements (with continuously reinforced concrete pavement below the surface, BOC), continuously reinforced concrete (CRC), and jointed concrete pavements (JCP). Additionally, updated cost estimates per mile for each treatment are available for each road category. The

decision process is a two-phase approach (Figure 34). In 2008, this two-phase approach was modified to include structural condition and truck traffic volumes, and the enhanced decision tree was integrated into the process. One of the main features of the approach is that the addition of the pavement structural information did not alter the core of the decision process already in place but provided an additional step that can be used when pavement structural condition is available. If structural information becomes unavailable, the decision process can revert to the core process already in place. VDOT currently uses the following five treatment categories (from do nothing to heavier treatments): Do Nothing (DN), Preventive Maintenance (PM), Corrective Maintenance (CM), Rehabilitation Maintenance (RM), and Reconstruction (RC). At the preliminary treatment stage, one of these five categories is selected based on the condition index and the decision matrices. In the enhanced decision process, based on the structural condition (and traffic level and construction history), the selected preliminary treatment can be either retained or modified to a heavier or lighter treatment.

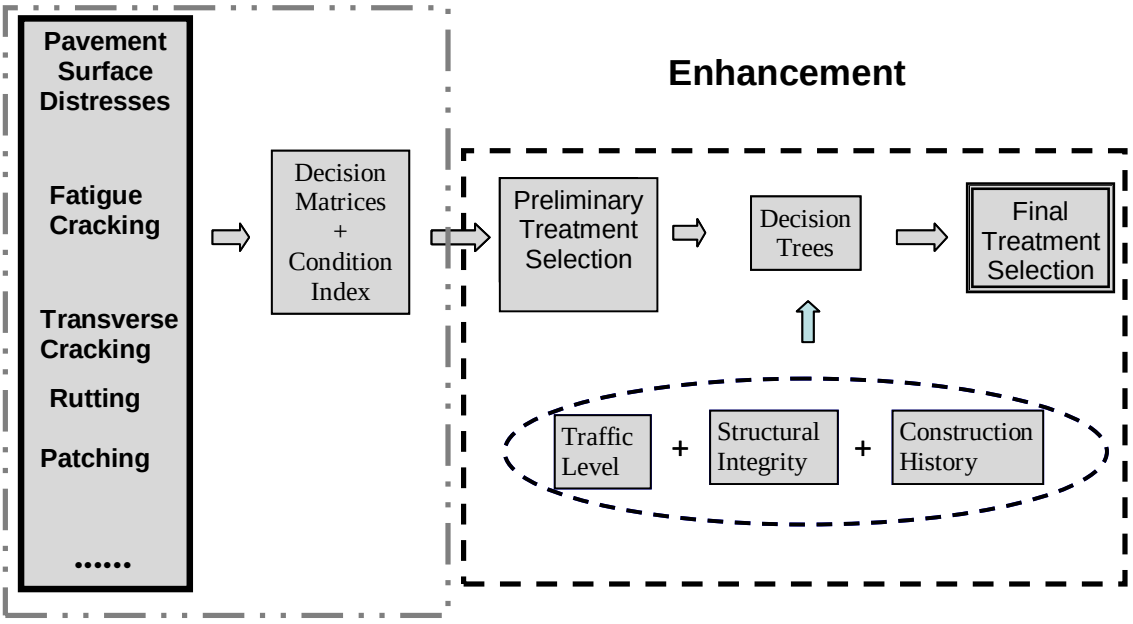

Figure 34. DOT two-phase decision process (Virginia Department of Transportation, 2008).

Example of PMS Decision Process with TSD-Derived Structural Condition

This section presents an example of how the structural condition will affect the triggered maintenance category at the network-level analysis for the tested I-81 section in Virginia. The approach is based on the CCI recommended treatment used by VDOT. It should be noted that in the actual VDOT decision process, the different distresses—e.g. cracking, rutting, etc.—are used to trigger the maintenance category and the CCI is used as an additional filter. Here the process is simplified for a clearer exposition. Figure 35 shows the maintenance categories as a function of CCI for the different road systems used by VDOT. This example uses I-81 and therefore the triggered categories for the interstate road system are used. The different treatment categories are

codified with a numerical value as follows: DN = 1, PM = 2, CM = 3, RM = 4, and RC = 5. After the triggered maintenance category is obtained from the CCI, the structural condition information is used to potentially bump up the triggered maintenance category. The structural condition information used is the one obtained from the SCI300 with thresholds determined from Table 2. The approach to bump up the triggered maintenance category is as follows: if all the SCI300 measurements in the pavement section have good structural condition, keep the maintenance category triggered by the CCI with a maximum category of 3; if there are SCI300 measurements within the pavement section that are classified as fair, bump up the maintenance category triggered by the CCI by one not to exceed a maintenance category of 5; if there are SCI300 measurements within the pavement section that are classified as poor, bump up the maintenance category triggered by the CCI by two not to exceed a maintenance category of 5 and a minimum category of 4. In total there are 747 0.1-mile sections tested in I-81.

The triggered maintenance categories obtained before and after taking into account the structural condition are shown in Figure 36. Of the 747 sections, 66 (8.8%) had the triggered maintenance category bumped up; 50 by one, and 16 by 2. The total number of sections in each maintenance category before and after incorporating the structural condition are DN 384 before, 345 after; PM: 338 before, 347 after; CM: 6 before, 25 after; RM: 14 before, 23 after; RC: 5 before, 7 after. The number of sections in the DN categories decreased, while the number of sections in all other categories increased. Again, this example is simplified, and other factors such as traffic level and pavement age can be considered (as is done by VDOT). It is expected that different state highway agencies will tailor their approach for their specific needs.

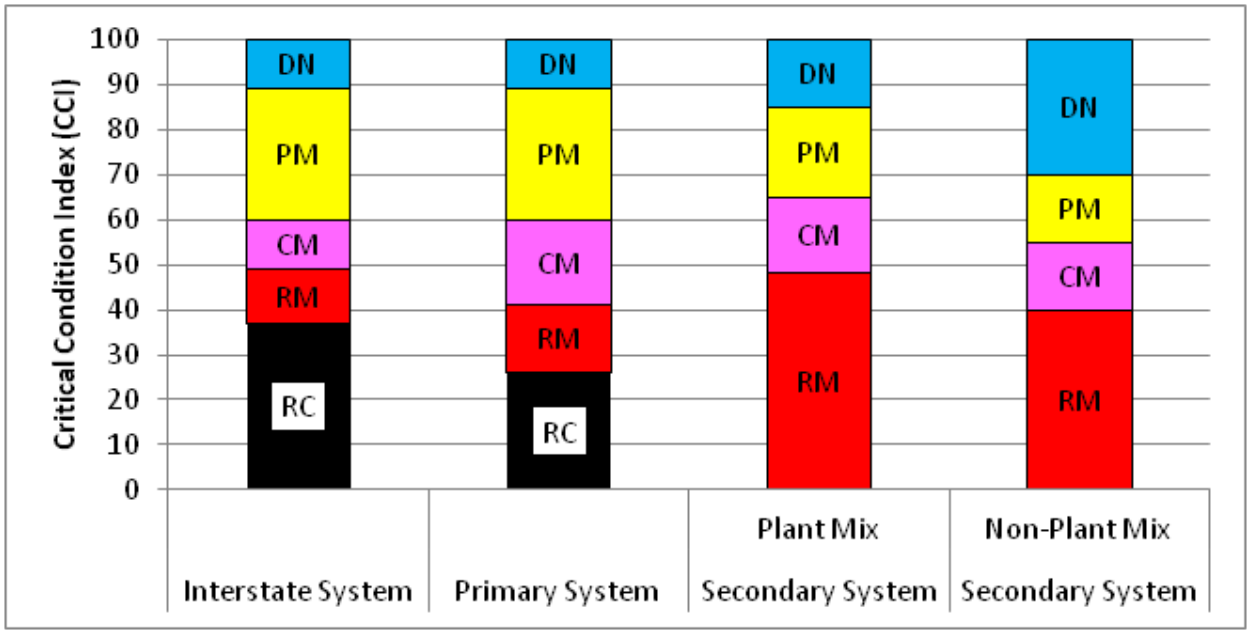

Figure 35. Maintenance activities for each road system (from Chowdhury, 2008).

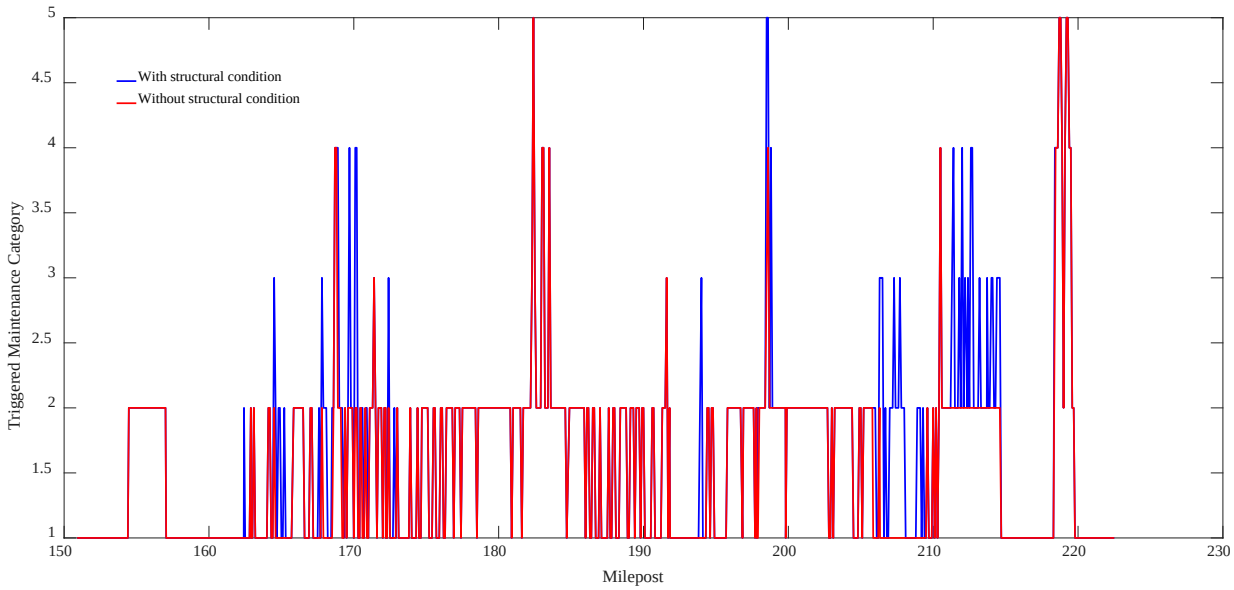

Figure 36. Triggered maintenance category before and after structural condition consideration.

CONCLUSION

This report summarizes the results of TSD testing performed in Virginia. The report focuses on answering the following important questions:

1. What is the TSD and what does it measure?
2. What is the structural condition of the tested roads?
3. How repeatable are TSD measurements?
4. How do TSD measurements compare with FWD?
5. How do TSD measurements compare with PMS data?
6. How can we use the information obtained from TSD measurements?
7. How can we incorporate TSD measurements into a PMS?

A summary of the answers to these questions follows.

1. **What is the TSD and what does it measure?** The TSD is an articulated truck with a loaded rear-axle that can measure the pavement structural condition at or near the traffic speed. Unlike the FWD, the TSD is a moving device (the FWD is stationary) and measures the deflection slope (the FWD measures the deflection) from which the deflections can be indirectly calculated.

2. **What is the structural condition of the tested roads?** Most tested roads had a structural condition classified as good. Most Fair and Poor condition were observed in secondary roads especially in the secondary roads tested near Petersburg. The structural condition of the tested roads was summarized in box plots showing the median, 50% range, and 90%

range of SCI300. These give a quick overview of the pavement condition. Color coded Google Earth figures for pavements estimated to be in Good, Fair, and Poor conditions are also provided showing the overall pavement condition of the tested roads.

3. **How repeatable are TSD measurements?** Repeated TSD measurements on U.S. 29 followed similar trends for SCI300. There was, however, some difference with the first set of measurements having slightly larger SCI300 values.

4. **How do TSD measurements compare with FWD data?** TSD measurements were compared with FWD measurements on I-81 and I-95. Both sets of measurements followed the same trends. The comparison between the two tests was limited to trends, because of expected difference in measurements due to the difference in loading configuration, and tested time and temperature. In terms of identifying the same weak sections, agreement between TSD measurements and FWD measurements was found to be reasonable and even better than the agreement between two different sets of FWD measurements.

5. **How do TSD measurements compare with PMS data?** Comparing TSD data with the surface condition (AC cracking, LDR, and CCI) obtained from the PMS data found that for each of the three tested interstate roads, the structural condition is not highly correlated with surface condition. However, comparing I-95 data with I-81 data in general, I-81 which was in a better structural condition (lower SCI), experienced lower fatigue cracking than I-95. This points to the fact that structural condition affects the development of fatigue cracking however, the observed surface cracking (or surface distress in general) is not a good predictor of pavement structural condition. A similar observation was made between TSD estimated structural number and LDR.

6. **How can we use the information obtained from TSD measurements?** TSD measurement information can help to better manage pavement sections. TSD measurements was used to identify strong and weak sections. The comparison with the FWD showed that identified weak and strong sections are compatible with FWD-identified sections. Furthermore, TSD measurements clearly identified tested bridges as strong pavement sections, as would be expected. An approach to estimate the remaining fatigue life of the pavement based on estimated temperature-corrected strains using the method developed by Rada et al. (2016) was also illustrated.

7. **How can we incorporate TSD measurements into a PMS?** VDOT already uses structural information obtained from FWD measurements in two-stage PMS approach. In the first stage, the triggered maintenance category in the PMS is based on surface condition. In the second stage, the triggered maintenance category is combined with structural condition information to determine the final recommended maintenance category. An example of the two-stage approach on 741 0.1-mile sections on I-81 is presented, and a total of 66 sections had the final suggested maintenance category bumped

up from the original triggered maintenance category based solely on pavement surface condition.

REFERENCES

AASHTO (1993). AASHTO Guide for Design of Pavement Structures, American Association of State Highway and Transportation Officials, Washington, D.C.

Asphalt Institute. (1982). Research and Development of the Asphalt Institute's Thickness Design Manual (MS-1) (Research Report No. 82-2). 9th edition.

Bryce, J., Flintsch, G.W., Katicha, S., and Diefenderfer, B. (2013). *Network-Level Structural Capacity Index for Network-level Structural Evaluation of Pavements,* Final Contract Report VCTIR 13-R9, Virginia Center for Transportation Innovation and Research, Charlottesville, VA.

Finn, F.N., Saraf, C., Kulkarni, R., Nair, K., Smith, W., & Abdullah, A. (1977). The use of distress prediction subsystems for the design of pavement structures. Proceedings of the 4th International Conference on the Structural Design of Asphalt Pavements (pp. 3–38), Vol. I, August. Ann Arbor, MI: University of Michigan.

Flintsch, G.W., Katicha, S.W., Bryce, J., Ferne, B., Nell, S., and Diefenderfer, B. (2013). *Assessment of Continuous Pavement Deflection Measuring Technologies,* Second Strategic Highway Research Program (SHRP2) Report S2-R06F-RW-1, The National Academies, Washington, D.C.

Flora, W. (2009). *Development of a Structural Index for Pavement Management: An Exploratory Analysis*, Master's Thesis, West Lafayette, Indiana: Purdue University.

Horak, E. (1987). "The use of surface deflection basin measurements in the mechanistic analysis of flexible pavements," *Proceedings of the Sixth International Conference Structural Design of Asphalt Pavements*, Vol. 1, University of Michigan, Ann Arbor, Michigan, USA.

Katicha, S.W., Ercisli, S., Flintsch, G.W., Bryce, J., and Diefenderfer, B. (2016). *Development of Enhanced Pavement Deterioration Curves,* Final Contract Report VCTIR 17-R7, Virginia Center for Transportation Innovation and Research, Charlottesville, VA.

Pedersen, L., Hjorth, P. G., and Knudsen, K. (2013). *Viscoelastic Modelling of Road Deflections for use with the Traffic Speed Deflectometer*. Kgs. Lyngby: Technical University of Denmark. (IMM-PHD-2013; No. 310).

Rada, G. R., Nazarian, S., Bisintine, B. A., Siddharthan, R.V., and Thyagarajan, S. (2016). *Pavement Structural Evaluation at the Network Level: Final Report,* FHWA-HRT-15-074,

Federal Highway Administration, McLean, Virginia, USA. https://www.fhwa.dot.gov/pavement/pub_details.cfm?id=1000

Rohde,G.T. (1994) “Determining pavement structural number from FWD testing”, *Transportation Research Record* no. 1448, Washington DC.

Virginia Department of Transportation. (2008). *Supporting Document for the Development and Enhancement of the Pavement Maintenance Decision Matrices Used in the Needs Based Analysis*. Richmond, VA.

Thyagarajan, S., Sivaneswaran, N., Petros, K., and Muhunthan, B. (2011). “Development of a simplified method for interpreting surface deflections for in-service flexible pavement” ICMPA129.